A Szilikátipari Tudományos Egyesület lapja

építőanyag

Journal of Silicate Based and Composite Materials

A TARTALOMBÓL:

2023/4

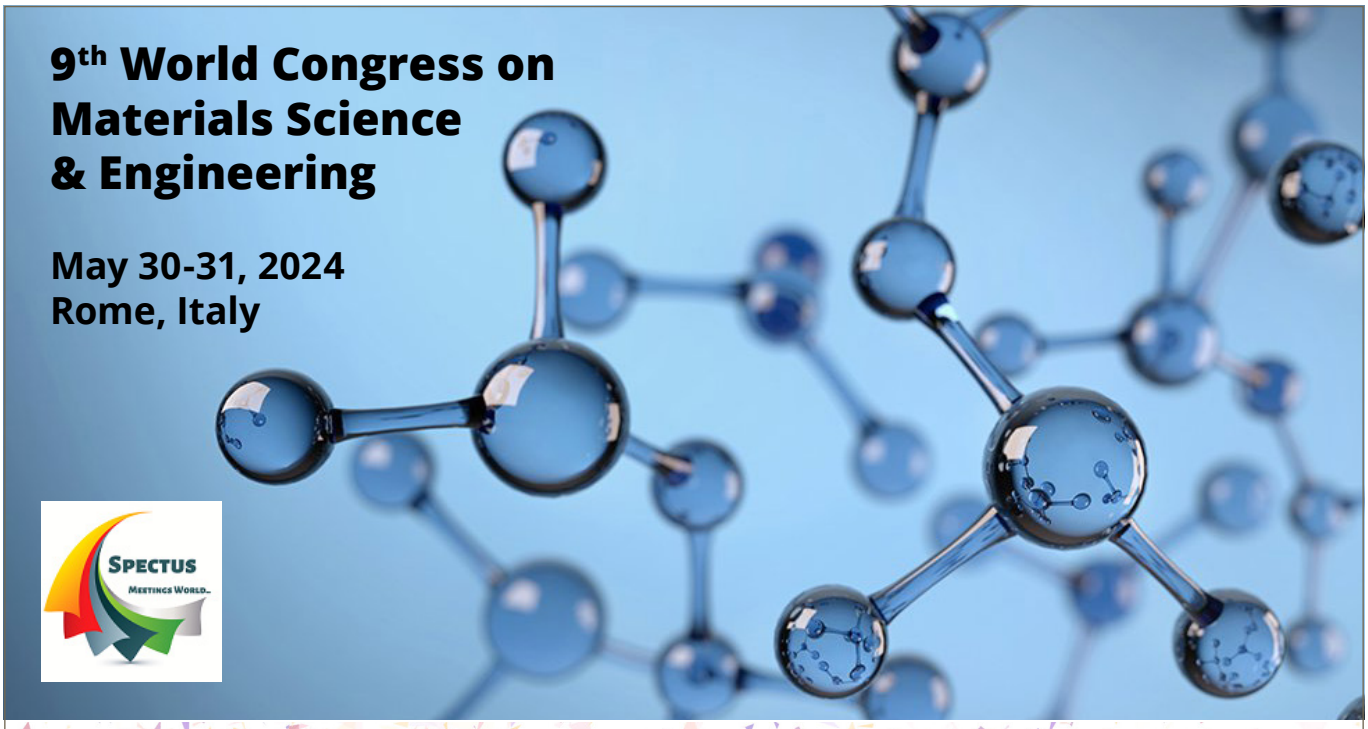

9th World Congress on Materials Science & Engineering

May 30-31, 2024
Rome, Italy

About the Conference

Material Science 2024 Heart fully welcomes every one of the members from everywhere the globe to join the 9th World Congress on Materials Science and Engineering. This year's event will be held on May 30-31, 2024 which is scheduled at the beautiful city of Rome, Italy. The main theme: Innovative Approach and Recent Developments in Materials Science and Engineering.

The MATCON 2024 will be a 2 days event that means to gather the key players of the Materials Science and Engineering community and related sectors. This event is launched with the aims to become an established event, attracting global participants, intent on sharing, exchanging and exploring new avenues of Materials Science and Engineering related scientific and commercial developments.

We will be really glad if you could join with us at Rome Italy or virtually from your place as it is hybrid event. Materials Science 2024 will be a platform of interactions for experts around the world and aims to accelerate scientific discoveries.

This conference includes keynote presentations, oral presentations, plenary talks, young research forums, poster presentations, student forum, technical workshop, symposia, start-up opportunities and meet the professors sessions. The scientific program features world-renowned experts and aspiring young researchers.

Looking forward to see you soon at Rome Italy during May 30-31, 2024.

spectusconferences.com/materials-science-conference

építőanyag
Journal of Silicate Based and Composite Materials
2023/4

TARTALOM

CONTENT

A finomkerámia-, üveg-, cement-, mész-, beton-, tégla- és cserép-, kő- és kavics-, tűzállóanyag-, szigetelőanyag-iparágak szakmai lapja
Scientific journal of ceramics, glass, cement, concrete, clay products, stone and gravel, insulating and fireproof materials and composites

A folyóiratot referálja · The journal is referred by:
ProQuest · Google Scholar · INDEX COPERNICUS INTERNATIONAL · THOMSON REUTERS
A folyóiratban lektorált cikkek jelennek meg.
All published papers are peer-reviewed.
Kiadó · Publisher: Szilikátipari Tudományos Egyesület (SZTE)
Elnök · President: ASZTALOS István
1034 Budapest, Bécsi út 120.
Tel.: +36-1/201-9360 ▪ E-mail: epitoanyag@szte.org.hu
Tördelő szerkesztő · Layout editor: NÉMETH Hajnalka
Címlapfotó · Cover photo: SIMON Andrea

WWW.EPITOANYAG.ORG.HU
EN.EPITOANYAG.ORG.HU

Online ISSN: 2064-4477
Print ISSN: 0013-970x
INDEX: 2 52 50 ▪ 75 (2023) 129-165

Glass foam experiment with eggshell as foaming agent and red mud as additive material

Ildikó FÓRIS ▪ University of Miskolc, Faculty of Earth and Environmental Sciences and Engineering, Institute of Raw Material Preparation and Environmental Technology ▪ ildiko.foris@uni-miskolc.hu
Gábor MUCSI ▪ University of Miskolc, Faculty of Earth and Environmental Sciences and Engineering, Institute of Raw Material Preparation and Environmental Technology ▪ gabor.mucsi@uni-miskolc.hu

Érkezett: 2023. 08. 10. ▪ Received: 10. 08. 2023. ▪ https://doi.org/10.14382/epitoanyag-jsbcm.2023.18

Abstract

Glass foam tablets were produced from green, brown, and white glass bottles, eggshell was used as foaming agent, Na-bentonite as binder and red mad as additive material.

Each tablet was 10 g and contained 2.5% Na-bentonite and 0.1% eggshell and different content of red mud (0-40 wt%), the rest of the mixture was glass powder. The ground raw materials were homogenized and pressed into glass foam tablets at 30 MPa using a hydraulic piston press.

The obtained glass tablets were heat treated at different temperatures. The study shows the chemical compositions of the raw materials, the specimen density of tablets before and after heat treatment, abrasion resistance and falling test of the tablets. From the results it can be concluded that the addition of red mud can reduce the foaming temperature to 800 °C from 900 °C, even at 1 wt% of red mud content. In this case a significant reduction in specimen density was observed from 1.33 g/cm^3 to 0.33 g/cm^3. Since the aim is to have a porous, lightweight product suitable for insulation, the specimen density value is important.

Keywords: recycling, glass foam, glass waste, eggshell waste, red mud, pressure agglomeration
Kulcsszavak: újrahasznosítás, üveghab, üveg hulladék, tojáshéj hulladék, vörösiszap, nyomással történő agglomeráció

Ildikó FÓRIS
PhD student at the University of Miskolc, Faculty of Earth and Environmental Sciences and Engineering, Institute of Raw Material Preparation and Environmental Processing. Her main fields in research are mechanical preparation, especially by fine grinding and utilization of waste materials as glass foams.

Gábor MUCSI
Associate Professor and Dean at the University of Miskolc, Faculty of Earth and Environmental Sciences and Engineering, Institute of Raw Material Preparation and Environmental Technology. His main fields in education and research are mechanical processes – comminution, especially fine grinding, mechanical activation, and utilization of industrial by products and waste materials. He has more than 100 publications.

1. Introduction

According to the Circular Economy Directive set by the European Union, 75% of glass waste should be recycled by 2035. This rate is much lower in Hungary, based on the latest known data which is 36%. The main cause of the problem in Hungary is that there is no domestic glass factory that would accept the generated amount of glass waste [1]. One way of recycling glass is glass foam. Glass foam production can be incorporated into the circular economy method, since 100% of the glass can be recycled, besides that other type of wastes can be used also during the process, such as eggshell waste and red mud creating high added-value products with less energy and raw material consumption [2].

Environmentally friendly insulation materials such as glass foams are gaining ground due to the wide spread of green technologies. Glass foams are used in the field of thermal and acoustic insulation in the construction industry [3, 4]. Glass foams are porous, lightweight materials (>80 V/V%) of gas and solid phase, they have inorganic chemical structure, relatively low transport costs, and they are easy to handle and combined with concrete [4, 5]. They are made from glass powder and foaming agent. After homogenization of the mixture the next step is heat treatment at high temperature in the range of 700-900 °C [6]. During the heat treatment the furnace reaches higher temperatures where gas formation occurs, and the glass viscosity is less than 106.6 Pa.s. The particles of the foaming agent are wrapped by the softened glass until the decomposition or reaction temperature of the foaming agent is reached, and releases gases that form bubbles in the softened glass. The glass viscosity and the surface tension decrease with the increasing temperature. The glass decreases the pressure over the gas bubbles and increases the expansion, which leads to the coalescence of the pores because of surface tension reduction [7, 8].

The combination of these properties makes glass foam suitable for a large-scale of applications in the construction industry.

Most of the glass waste is derived from mixed container glass bottles, window glass, or other types of glasses such as cathode ray tubes (CRT) in industrial glass foam production [9-11].

The goal of this paper is to produce high-added-value products with low-cost raw materials such as recycled glass bottles, eggshell waste, and red mud.

2. Materials and methods

Different colors of container glass bottles were used as the basis for glass foam tablets, eggshell waste as foaming agent, Na-bentonite as binder material and red mud as additional material. The main constituent of eggshell is calcium carbonate (94-96 wt%), and due to the high carbonate content, it is suitable for foaming because CO_2 is generated during the thermal decomposition of calcium carbonate at high temperature, which cause the forming porous structure of glass foam tablets. Several studies showed [12-15], that if red mud which is an alkaline leaching waste was added to the glass foam ceramics lower temperature was required during the foaming process, so in the end of the production less energy consumption required. Short terms used for sample materials in results and discussion part: ES – eggshell and RM – red mud.

The glass was prepared by crushing with a roll crusher with a screen size of 1 mm, then milling with a ball mill using stainless steel balls (Ø 20 mm) for 180 min under dry conditions to achieve the optimal particle size of the glass, which is < 100 μm because in other cases the foaming process will not be sufficient [16-19].

The foaming agent was milled for 120 minutes in a ball mill under dry condition with ceramic grinding balls (Ø 30 mm), and in the case of binder material and red mud which was additional material; no grinding was required because their particle size was in the fine size range. It was necessary to remove the organic content of the eggshell before milling, so it was heat treated in boiling water for 30 minutes.

Chemical compositions of glass powder, eggshell and red mud were measured by X-ray fluorescence (XRF) analysis.

The raw materials were sieved through a 32 μm opening sized sieve under wet conditions. This was necessary for each material to fall in the same size range, so the pore structure of the glass foam tablets was homogeneous.

The ES as foaming agent was added to the glass powder in 0.1 wt% and 2.5 wt% Na-bentonite as a binder material. The RM as additive was added to the tablets in different ratios: 0% (this contained only ES), 1 wt%, 5 wt%, 10 wt%, 20 wt%, 30 wt%, 40 wt%. The rest of the mixture were glass powder depended on the foaming agent, additive material, and binder material ratios. The tablets were prepared with a hydraulic piston press at 30 MPa pressure. Each tablet was 10 g.

The obtained raw tablets were heat treated in Nabertherm L (T) 3 laboratory static furnace at different temperature (700 °C, 800 °C and 900 °C) with 120 minutes residence time (furnace heating time 90 min +30 min residence time) using different heating rate (7,66 min, 8,77 min, 10 min).

The specimen density (ρ_s) of the tablets before and after heat treatment was determined by their geometrical measurements, using a calliper and their masses with an analytical balance.

The abrasion resistance of the products was measured in a laboratory ceramic-lined mill. 30 g from each RM ratio were tested. The 30 grams of material remained in the machine at 30 rpm for 10 minutes, and after removing the material, the fine fraction was sieved using a sieve with 1 mm opening size. From the mass of the fine fraction and the feeding material, the degree of abrasion was calculated using *Eq. 1*, where Δm_{abr} is the amount of abrasion (%), m_{fine} is the amount of material passed through the 1 mm sieve (g), and m_{feed} is the feeding material (30 g).

$$\Delta m_{abr} = \frac{m_{fine}}{m_{feed}} \cdot 100[\%] \quad (1)$$

For each of the RM contents, falling test was carried out to test the strength of the tablets. Each tablet was dropped from a height of 2 m with its edge until it broke, the number of drops was recorded.

3. Results and discussion

3.1 XRF results

Table 1 shows the chemical composition of the raw materials.

Eggshells have a high content of CaO which leads CO_2 formation during the foaming process. Glass contained high amounts of SiO_2, CaO and Na_2O. These results showed that these are typical soda-lime glasses. Red mud was Al- and Si-rich material because according to the results had a relatively high SiO_2 and Al_2O_3 content.

3.2 Density measurements

At 700 °C, it is clearly visible that the specimen density was reduced minimally compared to the pre-foaming condition, no significant foaming was observed (*Fig. 1*). At 800 °C and 900 °C, a significant decrease in specimen density occurred for tablets containing 0-5 wt% RM (*Fig. 2-3*). The addition of RM was done to reduce the temperature demand and thus make the process more energy efficient. From the results it can be concluded that RM is an effective additive material to decrease the temperature.

At both temperatures, the tablets containing 5 wt% RM had the lowest specimen density, 0.38 g/cm³ (at 800 °C) and 0.35 g/cm³ (at 900 °C).

The only significant change was seen in tablets containing 0 wt% RM, which contained only foaming agent. These tablets foamed at 800 °C but their specimen density was only 0.98 g/cm³, but after RM addition the value decreased to 0.47 g/cm³, even with 1 wt% addition. However, when 5 wt% RM was added to the tablets, the specimen density further decreased to 0.38 g/cm³. For tablets with RM content above 10 wt%, it was observed that their specimen density also increased linearly with the increasing RM content. This was observed in all temperature ranges, which clearly shows that the sintering intensity decreases with RM content above 10 wt%.

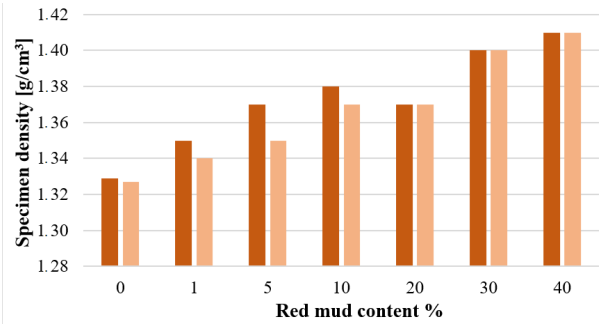

Fig. 1 Specimen density of tablets prepared at 700 °C before (dark orange) and after heat treatment (light orange) according to RM content
1. ábra A 700 °C-on készített tabletták testsűrűsége hőkezelés előtt (sötét narancssárga) és hőkezelés után (világos narancssárga) vörösiszap arány szerint

Unit	SiO_2 m/m%	Al_2O_3 m/m%	MgO m/m%	CaO m/m%	Na_2O m/m%	K_2O m/m%	Fe_2O_3 m/m%	MnO m/m%	TiO_2 m/m%	P_2O_5 m/m%	S m/m%	F m/m%	LOI m/m%
ES	0.3	0.0	0.62	54.4	0.13	0.13	0.03	0.001	0.002	0.499	0.21	<0.3	45.71
Glass powder	73.6	1.2	2.25	9.89	11.9	0.62	0.47	0.008	0.049	0.014	0.20	<0.3	-
RM	16.10	17.90	1.66	8.50	9.98	0.08	35.10	0,31	4.08	1.39	1.59	<0.3	12.8

Table 1 Chemical composition of raw materials
1. táblázat A nyersanyagok kémiai összetétele

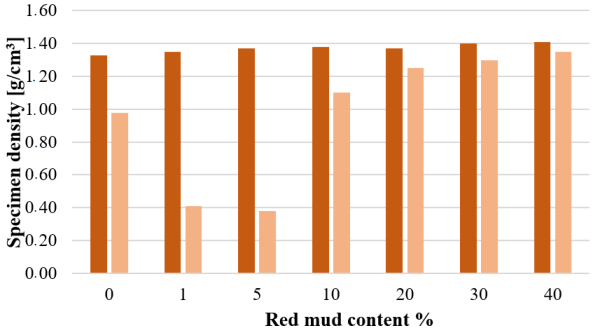

Fig. 2 Specimen density of tablets prepared at 800 °C before (dark orange) and after heat treatment (light orange) according to RM content
2. ábra A 800 °C-on készített tabletták testsűrűsége hőkezelés előtt (sötét narancssárga) és hőkezelés után (világos narancssárga) vörösiszap arány szerint

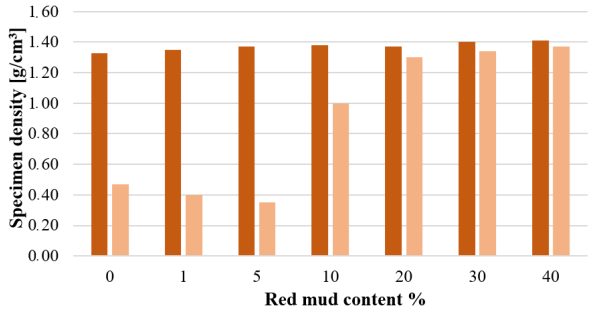

Fig. 3 Specimen density of tablets prepared at 900 °C before (dark orange) and after heat treatment (light orange) according to RM content
3. ábra A 900 °C-on készített tabletták testsűrűsége hőkezelés előtt (sötét narancssárga) és hőkezelés után (világos narancssárga) vörösiszap arány szerint

3.3 Abrasion test

The tablets with higher RM content showed higher abrasion, even though the abrasion rate was basically negligible for tablets. For the tablets containing only foaming agent, the highest abrasion was at 900 °C because the foaming mechanism was the highest level in this case in the three temperature ranges, where the specimen density was the lowest. This trend was also observed for the 1 and 5 wt% RM tablets. The smallest abrasion value was observed for the 10 and 20 wt% RM tablets at 700 °C, but there the foaming was not significant. This was followed in turn by tablets containing 1 wt% RM at 800 °C, where a significant decrease in specimen density was already observed compared to the density before heat treatment (*Fig. 1*). Overall, it can be concluded from the abrasion resistance test that the abrasion rate was below 2% at all temperatures.

Tablet type	Abrasion resistance value (%)		
	700 °C	800 °C	900 °C
0.1% ES	0.85	0.82	0.90
1% RM	0.78	0.72	0.74
5% RM	0.80	0.90	0.95
10% RM	0.70	0.78	0.75
20% RM	0.70	0.73	0.76
30% RM	0.80	0.81	0.79
40% RM	1.00	0.88	0.90

Table 2 Abrasion resistance values at different temperatures for each RM content
2. táblázat Kopásállóság értékei különböző hőmérsékleten az egyes vörösiszap tartalmak esetében

3.4 Falling test

From the falling test, the 700 °C tablets broke the fastest compared to the 800 °C and 900 °C tablets. It can be clearly seen from the results that tablets at 800 °C broke later at 1-10 wt% RM content than tablets at 900 °C, this may be since the decrease in specimen density was greater at 900 °C and thus greater foaming occurred, resulting in less compacted tablets and thus less breakage. The best value was obtained at 800 °C with 5 wt% RM, where the tablets withstood 20 falls, and at 900 °C, also with 5 wt% RM, with a value of 16 falls without breakage. It was observed that above 10 wt% RM the tablets broke sooner overall for all three temperature ranges. They were less mechanical resistant than tablets with less RM content, despite the higher foaming rate, resulting in a more porous structure, which could be a reason for the tablets breaking sooner.

Dropped tablet	Number of drops		
	700 °C	800 °C	900 °C
0.1% ES	8	12	12
1% RM	9	16	13
5% RM	10	20	16
10% RM	9	11	10
20% RM	7	10	7
30% RM	8	9	8
40% RM	7	10	8

Table 3 Falling test results for tablets prepared at different temperatures for each RM content
3. táblázat Ejtési vizsgálat eredményei különböző hőmérsékleten az egyes vörösiszap tartalmak esetében

4. Conclusion

From the preliminary experiments it can be concluded:

1. At 700 °C with 7.66 °C/min heating rate the specimen density of the tablets decreased minimally.
2. In the case of 800 °C and 900 °C with 8.77 °C/min and 10 °C/min heating rate the specimen density of the tablets containing 0-5 wt% RM significantly decreased because of the higher level of foaming.
3. Above 10% RM content, the tablets broke earlier during the falling test, so adding higher content of RM reduces mechanical strength of the tablets.
4. In addition, it was observed that tablets made at 900 °C with 0-5 wt% RM content broke earlier than those made at 800 °C, due to the higher foaming, even though there was no significant difference in specimen density reduction between the two temperatures. It can be concluded from the abrasion resistance test that the abrasion rate was below 2% at all temperatures.
5. The only significant difference between the tablets prepared at 800 °C and 900 °C was that although the tablets contained 0 wt% RM (contained only foaming agent). The resulting specimen density was significantly lower at 900 °C and foaming was more intense at 800 °C, which leads to the conclusion that the addition of RM can reduce the temperature demand and thus make the process more energy efficient.

5. Acknowledgement

„Supported by the ÚNKP-22-3 New National Excellence Program of the Ministry for Culture and Innovation from the Source of the National Research, Development and Innovation Fund."

Új Nemzeti Kiválóság Program
Kulturális és Innovációs Minisztérium

References

[1] Kálnai, G., Kálnai, M. (2007) Az üveghulladék gyűjtés, kezelés, hasznosítás helyzete Magyarországon. Human-Szervíz Kutató- és Munkakörnyezetfejlesztő Kft

[2] Scheffler, M., Colombo, P. (2006) Cellular Ceramics: Structure, Manufacturing. Properties and Applications https://doi.org/10.1002/3527606696

[3] Qi, Y., Xiao, X., Lu, Y., Shu, J., Wang, J. and Chen, M. (2019) Cathode ray tubes glass recycling: a review. *Science of The Total Environment,* 650, 2842–2849. https://doi.org/ 10.1016/j.scitotenv.2018.09.383

[4] Assefi, M., Maroufi, S., Mansuri, I. and Sahajwalla, V. (2021) High strength glass foams recycled from LCD waste screens for insulation application. *Journal of Cleaner Production,* 280, 1, 124311-124320. https://doi.org/10.1016/j. jclepro.2020.124311

[5] Cengizler, H., Koç, M. and Şan, O. (2021) Production of ceramic glass foam of low thermal conductivity by a simple method entirely from fly ash. *Ceramics International,* 47, 20, 28460-28470. https://doi.org/10.1016/j.ceramint.2021.06.265

[6] Spence, W. P. and Kultermann, E (2016) Construction Materials, Methods and Techniques. *Cengage Learning*, 510-526.

[7] da Silva R. C., Puglieri, F. N., de Genero Chiroli, D. M., Bartmeyer, G. A., Kubaski, E. T. and Tebcherani, S. M. (2021) Recycling of glass waste into foam glass boards: A comparison of cradle-to-gate life cycles of boards with different foaming agents. *Science of The Total Environment,* 771, 145276. https://doi.org/10.1016/j.scitotenv.2021.145276

[8] Østergaard, M.B., Petersen, R.R., König, J., Bockowski, M. and Yue, Y. (2019) Impact of gas composition on thermal conductivity of glass foams prepared via high-pressure sintering. *Journal of Non-Crystalline Solids,* X 1, 100014.

[9] Bueno, E. T., Paris, J. M., Clavier, K. A., Spreadbury, C., Ferraro, C. C. and Townsend, T. G. (2020) A review of ground waste glass as a supplementary cementitious material: A focus on alkali-silica reaction. *Journal of Cleaner Production,* 257, 120180. https://doi.org/10.1016/j.jclepro. 2020.120180

[10] Mucsi, G. Csőke, B., Kertész, M., Hoffmann, L. (2013) Physical characteristics and technology of glass foam from waste cathode ray tube glass, Journal of Materials, 1-11.

[11] Saparuddin, D. I., Hisham, N. A. N. H., Aziz, S. A., Matori, K. A., Honda, S., Iwamoto, Y. and Zaid, M. H. M. (2020) Effect of sintering temperature on the crystal growth, microstructure and mechanical strength of foam glass-ceramic from waste materials. *Journal of Materials Research and Technology,* 9, 3, 5640-5647. https://doi.org/10.1016/j. jmrt.2020.03.089

[12] Badanoui, A. I., Saadi, T. H. A. A., Stoleriu, S., Voicu, G. (2015) Preparation and characterization of fomaed geopolymers from waste and red mud. *Construction and Building Materials*, 84, 284-293.

[13] Chen, X., Lu, A., Qu, G. (2013) Preparation and characterization of foam ceramics from red mud and fly ash using sodium silicate as foaming agent. *Ceramics International*, 39, 1923-1929.

[14] Guo, Y., Zhang, Y., Huang, H., Meng, K., Hu, K., Hu, P., Wang, X., Zhang, Z., Meng, X. (2014) Novel glass ceramic foams materials based on red mud, *Ceramics International,* 40, 6677-6683.

[15] Xia, F., Gui, S., Pu, X. (2022) Performance study of foam ceramics prepared by direct foaming method using red mud and K-feldspar washed waste, *Ceramics International,* 48, 5197-5203

[16] Fernandes, H. R., Ferreira, D. D., Andreola, F., Lancellotti, I., Barbieri, L. and Ferreira, J. M. F. (2014) Ceramics International. 40, 8, 13371-13379., https://doi.org/10.1016/j.ceramint.2014.05.053

[17] König, J., Petersen, R. R. and Yue, Y. (2014) Influence of the glass-calcium carbonate mixture's characteristics on the foaming process and the properties of the foam glass. Journal of the European Ceramic Society, 34, 1591-1598

[18] König, J., Petersen, R. R. and Yue, Y. (2016) Influence of the glass particle size on the foaming process and physical characteristics of foam glasses. Journal of Non-Crystalline Solid, 447, 190-197. https://doi.org/10.1016/j.jnoncrysol.2016.05.021

[19] Attila, Y., Guden, M. and Tasdemirci, A. (2013) Foam Glass Processing Using a Polishing Glass Powder Residue. Ceramics International, 39, 5, 5869-5877., https://doi.org/10.1016/j.ceramint.2012.12.104

Ref.:
Fóris, Ildikó – **Mucsi**, Gábor: *Glass foam experiment with eggshell as foaming agent and red mud as additive material*
Építőanyag – Journal of Silicate Based and Composite Materials, Vol. 75, No. 4 (2023), 132–135. p.
https://doi.org/10.14382/epitoanyag-jsbcm.2023.18

The effect of the sintering temperature on the properties of the Al_2O_3-glass composites

SIMON Andrea ▪ Energia-, Kerámia- és Polimertechnológiai Intézet, Miskolci Egyetem ▪ andrea.simon@uni-miskolc.hu
KUROVICS Emese ▪ Energia-, Kerámia- és Polimertechnológiai Intézet, Miskolci Egyetem ▪ emese.mesterne@uni-miskolc.hu
MUCSI Gábor ▪ CERLUX Kerámia és Berendezésgyártó Kft. ▪ mucsig@cerlux.hu
KOCSERHA István ▪ Energia-, Kerámia- és Polimertechnológiai Intézet, Miskolci Egyetem ▪ istvan.kocserha@uni-miskolc.hu

Érkezett: 2023. 09. 20. ▪ Received: 20. 09. 2023. ▪ https://doi.org/10.14382/epitoanyag-jsbcm.2023.19

Kivonat

Manapság egyre nagyobb szerepe van az olyan kerámia anyagoknak, amelyek megfelelő szilárdsággal és jó villamos szigetelő képességgel bírnak, ugyanakkor relatíve alacsony hőmérsékleten szinterelhetők. Ilyen tulajdonságú kerámiák az üveg-kompozit kerámiák, melyek alacsony hőmérsékletű szinterelődését a báziskerámiához (ami általában alumínium-oxid) adagolt üvegpor biztosítja. Az üveg jellemzően olyan gondosan megtervezett oxidos összetételű fritt, amely 1000 °C alatt szinterelődik és olvad/lágyul. Ez a kompozit felhasználható a germicid lámpák lámpafejeinek a gyártásához is.

Egy kísérletsorozatot hajtottunk végre, amelyben egy ilyen üveg-kerámia kompozit tulajdonságainak változását vizsgáltuk meg az égetési hőmérséklet függvényében. A mintákat fröccsöntési technológiával állítottuk elő. Vizsgáltuk az égetett minták sűrűségét, porozitását, hajlító- és nyomószilárdságát, és hővezetési tényezőjét. A termékek morfológiáját és a keletkezett fázisokat is elemeztük az 1000 °C alatti ideális szinterelési hőmérséklet megtalálása érdekében.

Kulcsszavak: üveg-kerámia kompozit, szövetszerkezet, fröccsöntés, szinterelés
Keywords: glass-ceramic composite, microstructure, injection molding, sintering

SIMON Andrea
főállásban a ZF Hungary Kft.-nél dolgozik beszállítói fejlesztő mérnökként, részmunkaidőben pedig a Miskolci Egyetemen egyetemi docensként. 2010-ben szerzett PhD fokozatot a Miskolci Egyetemen. Jelenlegi kutatási témái az üveghabok, a hulladékok újrahasznosítása és a mikroszerkezeti jellemzés.

KUROVICS Emese
2022-ben szerzett PhD fokozatot a Miskolci Egyetemen, ahol tudományos munkatársként dolgozik a Kerámia- és Szilikátmérnöki Intézeti Tanszéken. 75 cikk szerzője vagy társszerzője.

MUCSI Gábor
Okl. anyagmérnök, kerámia- és szilikátmérnöki szakirány (Miskolci Egyetem 2012); A Cerlux Kerámia és Berendezésgyártó Kft. ügyvezető igazgatója (2020-). Érdeklődési területe: Al_2O_3 kerámiák nyersanyagelőkészítésének, összetételének fejlesztése és a késztermékre gyakorolt hatásának tanulmányozása; alacsony (~1000 °C) olvadáspontú műszaki kerámiák kutatása, gyártástechnológiájának fejlesztése. Hazai szakmai szervezetek tagja (SZTE; MAKESZ)

Kocserha István
a Miskolci Egyetemen szerzett diplomát, 2010 óta PhD fokozatot szerzett. Jelenleg a Miskolci Egyetem egyetemi docense és a Kerámia- és Szilikátmérnöki Intézeti Tanszék vezetője. Több mint 60 cikk és 1 szabadalom szerzője vagy társszerzője.

1. Bevezetés

Az emberi egészség megőrzése számos területen szükségessé teszi eszközök, felületek, légterek, használati vizek fertőtlenítését, csírátlanítását, melyet a nemrégiben lezajlott COVID járvány még inkább megerősített. Ennek egyik módja az úgynevezett germicid lámpák alkalmazása, melyek erős UV-C sugárzás létrehozásával vegyszermentesen képesek sterilizálni. A rövidhullámú ultraibolya sugárzás roncsolja a baktériumok DNS-t, működésekor ózon keletkezik, mely szintén fertőtlenítő hatású. Ezen lámpák szerkezeti eleme a lámpafej, lámpafoglalat, mely szigetelő anyagból kell készüljön. Ezen alkatrésszel szemben a megfelelő mechanikai és a villamos átütési szilárdság mellett követelmény az UV és ózonállóság, így egynemű vagy kompozit kerámia anyagból készül, mivel a sugárzás miatt műanyag itt nem alkalmazható [1-2].

A lámpafoglalat anyagának megfelelnek az üveg kerámia kompozit anyagok, melyek előállítása alacsonyabb hőmérsékleten történhet, mint pl. a tiszta alumínium-oxidól gyártott termékek esetén szükséges lenne.

Az üveg-kerámiai kompozitok jól szabályozható, egyedileg beállítható tulajdonságaik miatt egyre inkább kutatott anyagok a kerámiák világában [3-19]. Az üveg-kerámia kompozitokban a fő fázis egy magas szinterelési hőmérséklettel rendelkező dielektromos anyag [9]. A kristályos fázis biztosítja a megfelelő dielektromos tulajdonságokat. Az üvegfázis csökkenti a relatív permittivitást és növeli a dielektromos veszteséget, ugyanakkor a jelenlétének köszönhetően a szinterelési hőmérséklet csökkenthető (az üveg összetételétől függően) [9].

A kompozit zsugorodási folyamatát az üveg viszkózus áramlása és az alumínium-oxid/ üveg határfelületen végbemenő reakciók szabályozzák [3]. A szinterelés során az alumínium-oxid beoldódik az üvegbe, így annak összetétele megváltozik, és a tiszta üvegben kristályosodó krisztoballit, pszeudowollasztonit helyett más fázisok, pl. anortit, albit képződnek a határfelületi rétegben [3-5, 11, 14-15]. A krisztoballit képződése korlátozza a kerámia hordozó hatékonyságát, ha áramköri táblákon használják [17]. A krisztoballit képződésének megakadályozásához megfelelő mennyiségű (min. 10-20 V/V%) Al_2O_3 és legalább 900 °C hőmérsékletű szinterelés szükséges. A kristályosodás intenzitása a hőmérséklettel nő, azonban 1100 °C-os égetés esetén újra megnő az amorf fázis aránya [4-5]. 700 °C körüli hőmérsékleten történő égetés során az Al_2O_3 már részlegesen beoldódik az alacsony viszkozitású üvegfázisba, és az oldódás 800 °C-ig folytatódik. Az anortit fázis 875°C-on kezd az üvegfázisból kristályosodni az Al_2O_3 szemcsék felületén. Az anortit tömeghányada növekszik a hőmérséklet emelkedésével, amíg 950 °C vagy magasabb hőmérsékleten stabilizálódik [7]. Az Al_2O_3 részecskék hozzáadása akadályozza a krisztoballit képződését, mivel a szinterelés során Al^{3+}-ionok diffundálnak az üvegbe, és az Al^{3+}/ Al_2O_3 és az üveg Na^+/ K^+ ionjai között erős összekapcsolódás következhet be, ami az üveg szerkezetének és összetételének változásához vezet [8, 17-18].

Mivel az alumínium-ion üvegképzőként működik, az üvegben történő feloldódása csökkenti a nem kötő (non-bridging) oxigén-ionok mennyiségét, ami jelentősen növeli az üveg viszkozitását. Ez a jelenség egyre szignifikánsabbá

válik az alumínium-oxid szemcseméretének csökkenésével. Ebből következik, hogy az alumínium-oxid üvegben történő feloldódása megváltoztatja, lelassítja az üveg/alumínium-oxid kompozitok zsugorodását [3]. A zsugorodást az égetési hőmérséklet is jelentősen befolyásolja, 900-1100 °C között vizsgálva kezdetben növekszik a szinterelési hőmérséklettel, 1000 °C körül eléri a maximális értéket, majd csökken. Az olvadékfázisú szinterelés során a képződött üvegolvadék viszkozitása a hőmérséklet emelkedésével csökken, ami viszont a felületi feszültség változása következtében végbemenő átrendeződés miatt fokozza a tömörödést [6, 13]. 1000 °C felett a hőmérséklettel az alumínium-oxid beoldódása is egyre intenzívebb, ennek következtében nő az üvegolvadék viszkozitása, amitől a zsugorodáshoz szükséges szemcse-átrendeződés is lassabban megy végbe [6, 19-21].

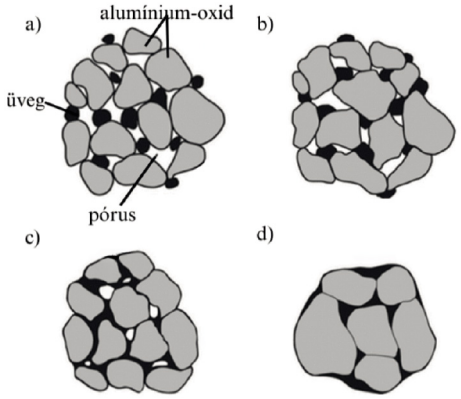

1. ábra A szinterelési folyamat sematikus ábrázolása: a) nyers üveg-alumínium-oxid kompozit, b-c) kevésbé zsugorodott szerkezet, d) jól tömörödött szerkezet [22]
Fig. 1 Schematic representation of the sintering process: a) raw glass-alumina composite, b-c) structure with less shrinkage, d) well-compacted structure [22]

A nyak korai megszilárdulása miatt kialakul egy szilárd alumínium-oxid-hálózat, amely magasabb hőmérsékleten lelassítja a tömörödést, mivel a váz széttörése nehéz az alumínium-oxidban gazdag, folyékony üveg fázis nagyon magas viszkozitása miatt (*1. ábra*) [6, 21]. Az üveg/kerámia kompozit azon a hőmérsékleten kezd tömörödni, ahol az üvegfázis viszkozitása kellő mértékben csökken, vagyis azon a hőmérsékleten, ahol az üvegolvadék képződik, mivel ezen hőmérséklet fölött a viszkózus áramlás elősegíti a további szinterelődését [7, 23-24]. Más tanulmányok szerint a maximális zsugorodás 800-900 °C közötti szintereléssel érhető el, a hőmérséklet további növelésével az égetett kompozitok sűrűsége csökken [10]. Kumar és társai szerint [15] a szinterelési hőmérsékletnek 1050 °C alatt kell lennie, hogy csökkentsék az Al_2O_3 felesleges oldódását az üvegben.

A megfelelő égetési hőmérséklet meghatározásánál tehát több szempontnak is érvényesülnie kell. Amennyiben LTCC (alacsony hőmérsékleten égetett kerámia/ low temperature cofired ceramic) alkalmazásra tervezünk anyagot, akkor az égetési hőmérsékletnek 950 °C alattinak kell lennie, hogy a beépített fém alkatrészek (pl. ezüst – 961 °C) olvadáspontját ne haladja meg, ugyanakkor a szerves komponensek maradéktalan eltávolításához legalább 800 °C szükséges [9]. Ez a hőmérséklettartomány korlátozza a felhasználható üvegek összetételét is, hiszen az alacsony lágyuláspontú üvegek (pl. boroszilikát) nem, vagy legalábbis önmagukban nem, csak egy magasabb lágyuláspontú üveggel kombinálva alkalmazhatók ilyen célokra.

Vizsgálatunkban szakirodalmi elemzés alapján, valamint itt nem részletezett előkísérletekben megállapított összetételű üveg-kerámia kompozitokhoz kerestük az lehető legalacsonyabb, 1000 °C alatti égetési hőmérsékletet, amely mellett a megfelelő fizikai-mechanikai tulajdonságok is biztosíthatók. Ehhez az elkészült mintákon pásztázó elektronmikroszkópos (SEM), röntgendiffrakciós (XRD), porozitás (Archimédesz-módszer), hővezető-képesség és hajlítószilárdság vizsgálatokat végeztünk, mely mérések az értékelés alapját adták.

2. Anyagok és módszerek

2.1 Próbatestek előállítása

A korábbi, itt nem részletezett előkísérletek során kiválasztott üveg-kerámia kompozit előállításához nagy tisztaságú alumínium-oxidot (Elektrokorund, IMERYS), üvegfrittet (FERRO), valamint paraffint és olajsavat használtunk fel. A porkeverék 2:1 arányú alumínium-oxid/üvegfritt keverékből állt, melyhez 4:1 arányban kevertük a fröccsöntést lehetővé tevő paraffin/olajsav keveréket. A fröccsmassza előkészítése felmelegített direktkeverőben történt 80 °C-on, beállított viszkozitás mellett. A tervezett vizsgálatoknak megfelelő, eltérő alakú és geometriai méretekkel rendelkező próbatestek előállítása a Cerlux Kft. saját fejlesztésű szerszámaival, valamint saját fejlesztésű alacsony nyomású fröccsöntőgépén történt. A fröccsöntési nyomás 6 bar, a fröccsöntő massza hőmérséklete 70 °C volt. A minták nyers geometriai adatait az *1.táblázat* mutatja be, a hajlítószilárdsági minták készítéséhez használt szerszám, valamint a fröccsöntött darabok egy égetőtokba helyezve az *2. ábrán* láthatóak.

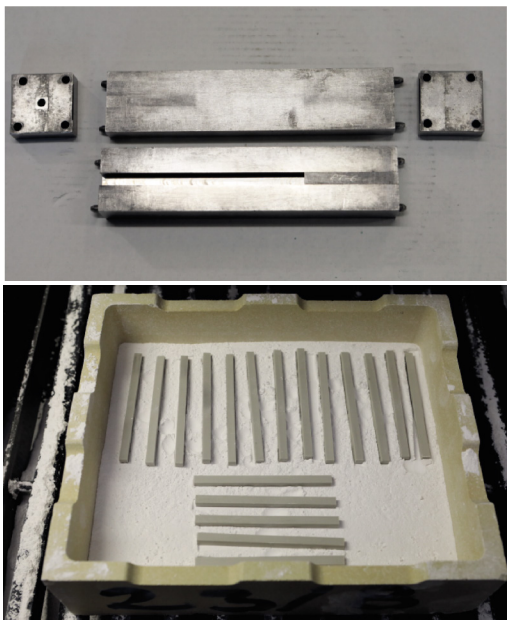

2. ábra Próbatest készítő szerszám a hajlítószilárdság vizsgálathoz, valamint a próbatestek az égetőtokban
Fig. 2 Specimen preparation tool for flexural strength testing, as well as the specimens in the firing aid

Vizsgálati minta	Átmérő	Magasság	Szélesség	Hossz
	mm	mm	mm	mm
Nyomószilárdság	10	11		
Hajlítószilárdság		6	6	100
Hővezetés	30	12		

1. táblázat A vizsgálati minták névleges méretei
Table 1 The nominal dimensions of test samples

Az elkészült próbatestekből az alakadást segítő kötőanyag eltávolítása 650 °C-on, 48 órás hőkezelési ciklussal történt földgázüzemű kemencében. A minták kiégetése egy optimális és minél alacsonyabb égetési hőmérséklet megtalálása érdekében hat különböző hőmérsékleten történt. Az elkészített próbatestek szinterelése tehát 850-900-950-1000-1050-1100 °C maximális hőfok mellett, 60 °C/óra felfűtési sebességgel egy Nabertherm HT 40/18 típusú laborkemencében történt. A hajlítószilárdság és a hővezetés mérésekhez a kiégetett próbatestek a *3. ábrán* kerülnek bemutatásra.

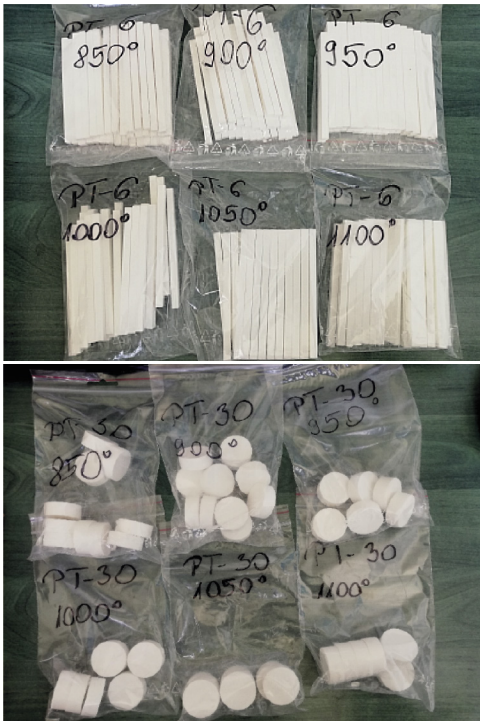

3. ábra Az elkészült és kiégetett minták egy része
Fig. 3 A part of the finished and fired samples

2.2 Mérési módszerek

A próbatestek gyártásához használt alumínium-oxid, valamint az üvegfritt szemcseméret eloszlásának megadásához Horiba LA-950 lézer granulométert használtunk. A kiindulási anyagok és a kiégetett próbatestek alkotó fázisainak meghatározásához Rigaku Miniflex II (Cu Kα, 2θ 3-90°) asztali röntgen diffraktométert, a fázisok kiértékeléséhez PDXL2 programot, a mennyiségi fázismeghatározáshoz pedig Rietveld teljes profillillesztéses eljárást alkalmaztunk. EDAX detektorral felszerelt ZEISS pásztázó elektronmikroszkóp segítségével megmértük az anyagok kémiai összetételét, valamint megfigyeltük a minták felületi morfológiáját. A hajlító- és a nyomószilárdság vizsgálatához alkalmas próbatestek eltérő geometriájú fröccsöntő szerszámban készültek. Az előbbi vizsgálathoz hasáb, míg az utóbbihoz hengeres mintákat használtunk. A mérések Instron 5560 univerzális húzó-nyomó berendezésen készültek. A hővezetési tényező meghatározásához csiszolt felületű, 30mm átmérőjű hengeres mintákat alkalmaztunk, és a tranziens sík-lap módszer elvén működő C-Therm TCi hővezető berendezést használtuk, a méréseket szobahőmérsékleten végeztük. Utóbbi két vizsgálatról készített felvétel a *4. ábrán* látható. A különböző hőmérsékleten égetett termékek porozitását vízfelvételi értékekből határoztuk meg. A vízfelvétel-vizsgálati metódusban 48 órás áztatást 3 órás forralás követett, ezután mértük az értékeket. Valamennyi statisztikai kiértékelést kívánó mérést 20 mintán végeztük el.

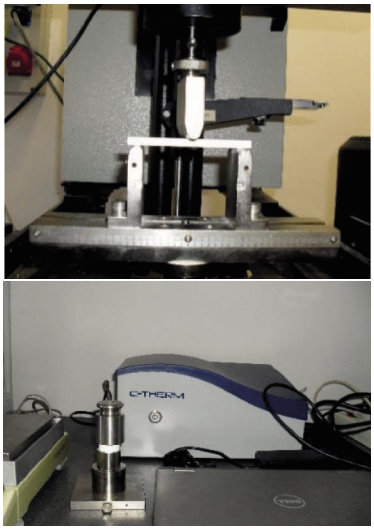

4. ábra Próbatest hajlítószilárdság vizsgálata és hővezetés mérése
Fig. 4 Examination of the flexural strength of the specimen and measurement of thermal conductivity

3. Eredmények

3.1 Az alapanyagok mérési eredményei

Az elvégzett röntgenvizsgálatok alapján a felhasznált alumínium-oxid alapanyagot alapvetően korund (Al_2O_3) alkotja, mellette kis mennyiségben jelen van diaoyudaoit ($NaAl_{11}O_{17}$) és hibonit ($CaAl_{12}O_{19}$), amelyek a korundgyártás során keletkező, mesterséges ásványok. A használt fritt teljes egészében amorf szerkezetű. Az alapanyagok oxidos összetétele és szemcseméret eloszlása a *2. táblázatban* található.

	Szemcseméret, μm				
	D90	D50	D10	Átlag	Medián
Elektro-korund	43,9	17,67	7,89	22,65	17,67
Fritt	22,54	10,52	4,34	12,33	10,50

	Oxidos összetétel, m/m%							
	Na_2O	MgO	Al_2O_3	SiO_2	ZrO_2	K_2O	CaO	ZnO
Elektro-korund	0,8		98,78				0,42	
Fritt	2,47	2,69	6,21	58,28	8,78	2,78	11,10	7,70

2. táblázat Az alapanyagok jellemző szemcseméretei és oxidos összetétele
Table 2 Typical grain sizes and oxide composition of the raw materials

Az anyagok kiindulási morfológiáját a *5. ábra* mutatja be. Mindkét anyagra határozott élekkel rendelkező, poliéderes szemcsealak jellemző, mind a durva, mind a finomabb frakció tekintetében.

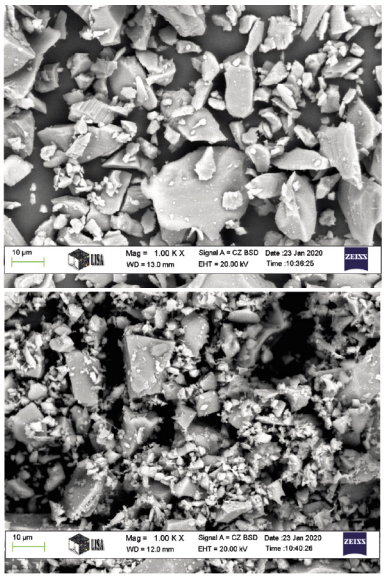

5. ábra A korund és a fritt minta SEM felvétele N=1000x
Fig. 5 SEM image of the corundum and frit sample N=1000x

3.2 Az égetési hőmérséklet hatása a termék tulajdonságaira

A 850-1100 °C közötti hőmérsékleten égetett üveg-kompozit mintákon elvégzett sűrűség, porozitás, zsugorodás, vízfelvétel és hővezetés, valamint a szilárdságvizsgálatok számszerű eredményeit a *3. táblázat* foglalja össze. A nyomó és hajlítószilárdsági vizsgálatok eredménye a *6. ábrán* kerül bemutatásra. Legnagyobb hajlító- és nyomószilárdsági értékkel a 950 °C-on égetett minták rendelkeztek. Érdekes, hogy a 950 °C feletti égetési hőmérséklet hatására kismértékben csökkent az átlagos nyomószilárdság, azonban nem tér el jelentősen a 850 °C-os égetett minták szilárdságától. A 900 °C-on égetett minták esetében azonban lényeges szilárdság csökkenés volt tapasztalható. A hajlítószilárdsági értékek 950 °C-ig közel változatlanok, majd 1000-1100 °C között 10-15%-kal csökkennek. Látható, hogy a hőmérséklet növelésével sem a nyomó, sem a hajlítószilárdsági értékekben nem következik be javulás. A *3. táblázat* tartalmazza a mérések szórását is, mely a nyomószilárdság értékek esetén 9-13%, míg a hajlítószilárdságok esetén 1000-1100 °C között a 8-12%-ról 23-27%-ra nő meg. Ezen értékekből tehát az látszik, hogy az égetés 1000 °C-alatt kedvezőbb.

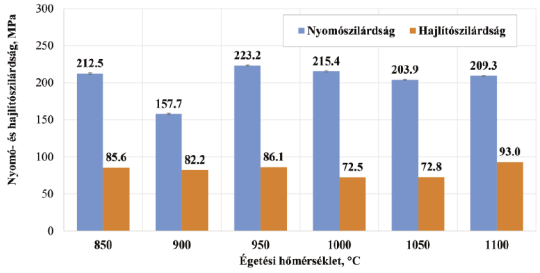

6. ábra A minták nyomó és hajlítószilárdsági értékei
Fig. 6 The compressive and flexural strength values of the samples

	Égetési hőmérséklet					
	850 °C	900 °C	950 °C	1000 °C	1050 °C	1100 °C
Zsugorodás átmérő, %	3,98	3,92	3,84	4,06	4,00	3,94
Zsugorodás hossz, %	5,42	4,08	5,41	5,37	5,20	5,05
Zsugorodás átlag, %	4,61	4,00	4,62	4,71	4,60	4,49
Vízfelvétel, %	11,00	10,8	10,7	11,00	11,4	11,20
Hővezetési tényező, W/mK	1,86	2,00	2,01	1,95	1,87	2,11
Nyomó-szilárdság, MPa	212,5	157,7	223,2	215,4	203,9	209,3
Szórás, %	9%	10%	13%	12%	10%	10%
Hajlító-szilárdság, MPa	85,6	82,2	86,1	72,5	72,8	93,0
Szórás, %	4%	12%	8%	27%	23%	13%

3. táblázat Az égetett minták mért értékeinek átlaga
Table 3 The average of the measured values of the sintered samples

A minták sűrűségi értékei, valamint a számolt porozitás értékek a *7. ábrán* kerülnek bemutatásra. A minták égetési átmérőben mért zsugorodás értékei nem térnek el jelentősen, a 950 °C és az 1000 °C-on hőkezelt minta közötti 5,5% volt a különbség. A minták magasság, illetve hosszmérete mentén a 900 °C-on égett minták zsugorodtak legkevésbé. Ezekhez hasonló tendencia mutatkozik a vízfelvétel és hővezetési tényező értékekben is. A sűrűséget nem befolyásolta a hőmérséklet, viszont a porozitás érték 950 °C-on a legkisebb, de ez is 5,5%-ban tér el a maximális, 1050 °C-on mért értéktől.

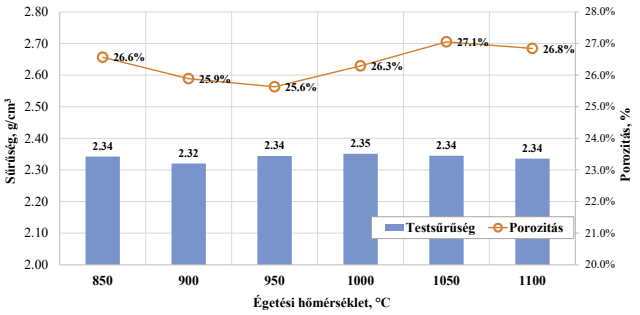

7. ábra A minták sűrűsége és porozitása a hőmérséklet függvényében
Fig. 7 Density and porosity of the samples as a function of temperature

3.3 Morfológia és fáziselemzés

A minták töretfelületének pásztázó elektronmikroszkópos megfigyelése és a készült képek elemzése kimutatta, hogy egy, a kötőanyag eltávolítása után visszamaradt pórusrendszer szövi át a mintákat. A pórusok szabálytalanul helyezkednek el, legnagyobb méretük néhány 10µm. A *8. ábra* mutatja be egy-egy 950 °C és 1000 °C-on égetett üveg-kerámia minta SEM felvételét. A szilárdsági adatokban jelentkező szórást, valamint a jelentős porozitás értékeket az elkészült felvételek alátámasztják. Az égetési hőmérséklet növelése nem okozott lényeges változást a minták töretfelületének morfológiájában.

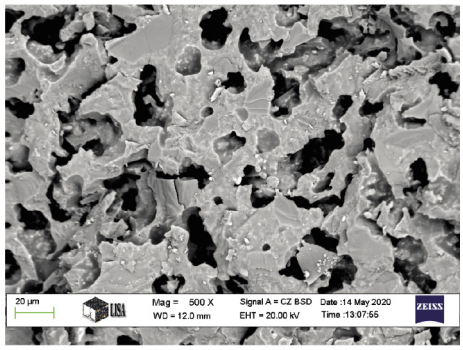

a)

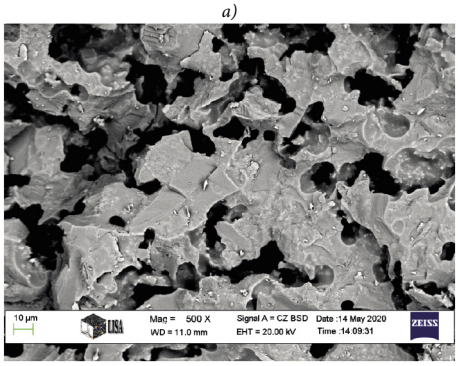

b)

8. ábra A 950 °C és 1000 °C-on égetett üveg-kerámia kompozitok szövetszerkezete
Fig. 8 The structure of glass-ceramic composites fired at 950 °C and 1000 °C

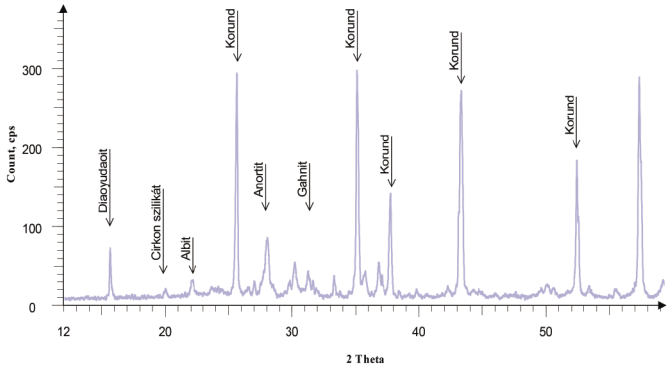

9. ábra Az égetett mintákban jelenlévő fázisok 850 °C-on
Fig. 9 Phases of samples sintered at 850 °C

A minták röntgendiffrakciós elemzése alapján a kiindulási kristályos korund fázis és az amorf fritt üveg fázis keverékéből a 850 °C-on égetett mintában már főként kristályos fázisok vannak jelen, mintegy 5% amorf tartalom mellett. Az azonosított fázisok: korund, albit, anortit, cirkonszilikát, gánit és a kiindulási mintában is meglévő diaoyudaoit fázis (*9. ábra*). Ezen fázisok megmaradnak 1100 °C-ig, azonban mennyiségük kismértékben változik. A 900 °C-on szinterelt mintában már egyértelmű a fritt olvadása, amely megnöveli a termékben az amorf fázis mennyiségét. Ezen a hőmérsékleten mintegy 22 m/m% mennyiség mutatható ki, mely 950 °C-on 16 m/m%-ra csökken, mely jelzi a kristályos fázis arányának növekedését.

3.4 Kísérleti üzemi gyártás

A kísérletek során fejlesztett 1000 °C alatt égethető üveg-kerámia kompozit keverékből, a sikeres kismintás kísérletek elvégzése után, kísérleti termékgyártásra is sor került a Cerlux Kft. telephelyén. A kísérleti termék elkészítéséhez, egy egyszerű termékgeometria került kiválasztásra. A gyártáshoz használt fröccsöntő szerszámot, valamint a termék geometriáját a *10. ábrán* mutatjuk be.

10. ábra A kísérleti termékhez használt fröccsöntő szerszám és a már elkészült termék
Fig. 10 The injection molding tool used for the experimental product and the finished product

A gyártás a Cerlux Kft. szintén saját fejlesztésű alacsony nyomású fröccsöntőgépén és saját fejlesztésű szerszámával történt. A fröccsöntési nyomás 6 bar, a fröccsöntő massza hőmérséklete 70 °C volt, 20 °C-os hűtővíz mellett. A *11. ábrán* a fröccsberendezés, valamint a nyers termékek kordierit égetőtokba helyezve láthatók. A mintákat timföldes megtámasztás mellett, gázüzemű kemencében 850 °C-on kerültek kiégetésre.

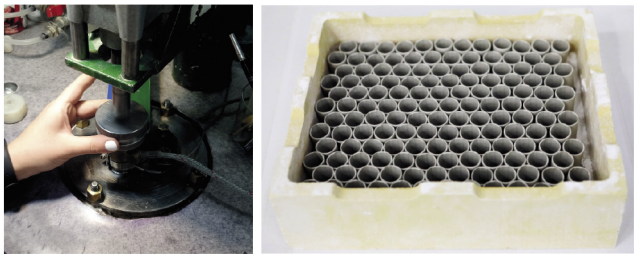

11. ábra A fröccsöntési művelet valamint az égetőtokba helyezett nyers termékek
Fig. 11 The injection molding operation and the raw products placed in the crucible

A kísérleti nyersgyártás során nem volt jellemző az átlagtól magasabb selejtképződés. Mivel a 850 °C-os égetési hőmérséklet adott volt, így a nagyobb mennyiségű minta esetén szükséges volt a megfelelő égetési görbe és hőntartási idő megtalálása annak érdekében, hogy a tokban lévő valamennyi termék megfelelő módon kiégjen. A megfelelőnek ítélt kísérleti égetés után a termékeket egyesével vizsgáltuk a végleges méret, zsugorodás, porozitás, felületi minőség és mázazhatóság szempontjából is. A mért értékek a 3. *táblázatban* foglaltaknak megfelelően alakultak. A termékek felülete megfelelő máztapadást biztosított a *10. ábrán* látható termék elkészítéséhez.

4. Konklúzió

Az elektrokorund és a fritt üveg által alkotott üveg-kerámia kompozit különböző hőmérsékleten végzett kiégetése alapján megállapítható, hogy a fritt olvadási képessége, valamint a kötőanyag kiégésének jellege hatással van a minták főbb, nem elektromos tulajdonságaira. A kísérletben használt 850-1100 °C-os tartományban a vizsgált jellemzők nem változtak számottevően, csak a 900 °C-os szinterelés esetén volt 5-10%-os nyomószilárdság és zsugorodása csökkenés. A vizsgált keverék

tehát akár 850 °C-on is égethető, hiszen a magasabb égetési hőmérséklet a fenti mérések alapján már nem okoz jelentős változást a tulajdonságokban.

5. Köszönetnyilvánítás

Jelen kutatómunka az Európai Regionális Fejlesztési Alap és Magyarország Kormányának társfinanszírozásával megvalósult GINOP-2.1.2-8-1-4-16-2017-00219 azonosító számú projekt eredményeként készült el. A szerzők köszönetet mondanak a Miskolci Egyetem, Anyag és Vegyészmérnöki Kar kollégáinak a vizsgálatok során nyújtott segítségéért.

Felhasznált irodalom

[1] T. K. Gachovska et al., „Design of Continuous Flow UVC Lamp for Office Air Germicide Elimination," 2021 IEEE Canadian Conference on Electrical and Computer Engineering (CCECE), ON, Canada, pp. 1-6, 2021. https://doi.org/10.1109/CCECE53047.2021.9569203

[2] Milad Raeiszadeh and Babak Adeli: A Critical Review on Ultraviolet Disinfection Systems against COVID-19 Outbreak: Applicability, Validation, and Safety Considerations, ACS Photonics Vol.7, No.11, pp.2941–2951, 2020. https://pubs.acs.org/doi/10.1021/acsphotonics.0c01245

[3] Yu-Ching Fang and Jau-Ho Jean: Effects of Alumina on Densification of a Low-Temperature Cofired Crystallizable Glass+Alumina System, Japanese Journal of Applied Physics Vol. 46, No. 6A, pp. 3475–3480, 2007.

[4] Jau-Ho Jean, Yu-Ching Fang, Steve X. Dai and David L. Wilcox, S: Effects of Alumina on Devitrification Kinetics and Mechanism of K_2O–CaO–SrO–BaO–B_2O_3–SiO_2 Glass, Jpn. J. Appl. Phys. Vol. 42 pp. 4438–4443 Part 1, No. 7A, 2003

[5] Gülsüm Meryem Dursun, Cihangir Duran: Glass alumina composites for functional and structural applications, Ceramics International Vol. 45 pp.12550–12557, 2019.

[6] Kostja Makarovič, Anton Meden, Marko Hrovat, Janez Holc, Andreja Benčan, Aleš Dakskobler, Darko Belavič, Marija Kosec: The Effect of the Firing Temperature on the Properties of LTCC, https://pdfs.semanticscholar.org/742a/32f8acadf54f52368387987f9f5f3584e38a.pdf, Letöltve 2020.03.16

[7] Suprapedi, Muljadi, Ramlan: Effect of Addition of Amorphous Glass (Soda Lime Glass) on Sintering Process and Properties of Alumina Ceramics, IOP Conf. Series: Journal of Physics: Conf. Series Vol. 1120, 012038, 2018.

[8] M.M.R.A. Lima, R.C.C. Monteiro, M.P.F. Graça, M.G. Ferreira da Silva: Structural, electrical and thermal properties of borosilicate glass–alumina composites, Journal of Alloys and Compounds Vol. 538 pp.66–72, 2012.

[9] M. M. R. A. Lima and R. C. C. Monteiro: Shrinkage Behaviour of Borosilicate Glass-Al_2O_3 Composites during Isothermal Sintering, Materials Science Forum Vols 514-516 pp 648-652, 2006.

[10] Bo Li, Yang Xu, and Shuren Zhang: The Size-Effect of Al_2O_3 on the Sinterability, Microstructure and Properties of Glass-Alumina Composites, Glass Physics and Chemistry, Vol. 41, No. 5, pp. 503–508., 2015

[11] M. Margarida. R. A. Lima és C. C. Monteiro: Viscous Sintering in a Glass-Alumina System, Materials Science Forum Vols. 587-588 pp. 143-147, 2008.

[12] I. Higby és James E. Shelby: Properties of Glass/Alumina Composites, Communications of the American Ceramic Society, C-229, 1983

[13] Qingshan Zhu, Gijsbertus de With, Leonardus J. M. G. Dortmans, Frits Feenstr: Near net-shape fabrication of alumina glass composites, Journal of the European Ceramic Society Vol. 25 pp.633–638, 2005.

[14] Qin Xia, Chao-Wei Zhong, Jian Luo: Low temperature sintering and characteristics of K_2O–B_2O_3– SiO_2–Al_2O_3 glass/ceramic composites for LTCC applications, J Mater Sci: Mater Electron Vol. 25 pp. 4187–4192, 2014.

[15] K. P. Kumar, V. C. S. Prasad, P. S. Mukherjee and P. G. Mukunda: Behaviour of Lead Borosilicate Glass/Alumina Composite in the Temperature Range 900-1100 °C, Materials Science and Engineering, B5 pp.1-4, 1989.

[16] M. T. Sebastian1 and H. Jantunen: Low loss dielectric materials for LTCC applications: a review, International Materials Reviews Vol. 53 No. 2, 2008.

[17] A.A. El-Kheshen: Effect of alumina addition on properties of glass/ceramic composite, British Ceramic Transactions Vol. 102 No. 5, 2003.

[18] Jau-Ho Jean, Chia-Ruey Chang, Ruey-Ling Chang, Tong-Hua Kuan: Effect of alumina particle size on prevention of crystal growth in low-k silica dielectric composite, Materials Chemistry and Physics Vol. 40 pp. 50-55 1995.

[19] R.C.C. Monteiro, M.M.R.A. Lima: Effect of compaction on the sintering of borosilicate glass/alumina composites, Journal of the European Ceramic Society Vol. 23 pp.1813–1818, 2003.

[20] P. Palanisamy, D.H.R. Sarma and R.W. West, J. Am. Ceram. Soc. Vol. 68 C215. 1985.

[21] BI-Shiou, W.-Y. Hsu and J.-G. Duh, Ceram. Int. Vol. 14 p.7, 1988.

[22] German, R.M., Suri, P. & Park, S.J. Review: liquid phase sintering. J Mater Sci Vol. 44, pp. 1–39, 2009. https://doi.org/10.1007/s10853-008-3008-0

[23] Kemethmüller, S., Hagymasi, M., Stiegelschmitt, A., Roosen, A.: Viscous Flow as the Driving Force for the Densification of Low-Temperature Co-Fired Ceramics, Journal of the American Ceramic Society, Vol. 90 No. 1 pp. 64-70, 2007.

[24] Cole, S., Wellfair, G., High temperature viscosity control in multi-layer glasses - a new concept, Proceedings of the ISHM Symposium, Boston, Massachusetts: 25-34, 1974.

Ref.:
Simon Andrea – **Kurovics** Emese – **Mucsi** Gábor – **Kocserha** István: *Az égetési hőmérséklet hatása az Al_2O_3-üveg kompozit tulajdonságaira*
Építőanyag – Journal of Silicate Based and Composite Materials, Vol. 75, No. 4 (2023), 136–141. p.
https://doi.org/10.14382/epitoanyag-jsbcm.2023.19

Calcined kaolinitic clay as a supplementary cementing material and its pozzolanic effect on concrete blends characteristics (Part I)

Nabil A. ABDULLAH
Consultant and Research Director in Aluminum Sulphate Co. of Egypt (ASCE). Ph.D. in Environmental science, Faculty of Science, Ain Shams University, Egypt.

Hajer N. Abdullah
Research assistant in October University for Modern Science and Arts (MSA university), Faculty of Engineering, Civil Engineering Department.

Nabil A. ABDULLAH ▪ Research & Development Dept. Director, Aluminum Sulphate of Egypt ▪ nabilxp9@gmail.com
Hajer ABDULLAH ▪ Civil Engineering Dept., MSA university, Egypt ▪ Hnabdullah@msa.edu.eg

Érkezett: 2023. 04. 25. ▪ Received: 25. 04. 2023. ▪ https://doi.org/10.14382/epitoanyag-jsbcm.2023.20

Abstract
The calcined kaolinitic clay (CKC) was investigated as a supplementary cementing material to assess its effect on the characteristics of concrete. The experimental protocol included optimization of the mixes of CKC/OPC containing 5, 10, 15, 20, 25, 30 and 35% CKC for production of hardened concrete. An evaluation of the use of CKC which contains about 79% of kaolinite mineral in south Sinai quarries in concrete fabrication. The objective of this study is to deliver an overview on CKC utilized in concrete modification. The physical and chemical characteristics of CKC were assessed. The compressive strength and slump of concrete was tested and discussed. The findings suggest that adding CKC to concrete enhances certain characteristics, particularly mechanical capabilities. For optimal performance, the right dosage ranged is between 10 to 20% by weight of the binder. The optimal replacement ratios for cement with CKC was 10% and 15%, which improved the compressive strength by an average of 120.8 and 118.7% respectively at the age of 28 days compared to the control mix. Assessment of the optimal dosage out of the two ratios (10 & 15%) requires a study of their fulfillment of many characteristics as well as their effect on durability and sustainability and their efficiency in facing harmful elements and media. And then determine the best ratio from the technical and economic point of view.
Keywords: kaolin, kaolinitic clay, calcined kaolin, metakaolin, pozzolanic materials, concrete mineral additives
Kulcsszavak: kaolin, kaolinites agyag, kalcinált kaolin, metakaolin, puccolán anyagok, beton ásványi adalékok

1. Introduction

Concrete fabrication and application in the building activity have increased due to its durability, and economic characteristics compared with other construction materials [1-3].

One ton of concrete is produced yearly by each human all over the world [4]. The production of Portland cement, has several disadvantages, including intensive energy demand and sharp environment pollution [5]. The calcination process emits huge amount of carbon dioxide due to the heating of limestone and the firing of petrol fuels for production of cement [6, 7]. Cement is the main ingredients in concrete since it needs water to bind the fine and coarse aggregates. Cement production was over 4 billion tons per year in 2018 and the demand is increasing, emitting great quantity of carbon oxides into the biosphere participating in the warming of the earth [8].

The use of supplemental cementitious materials (CMs) such as flied ash [9] fumed silica [10] waste glass [11] and ground granulated blast furnace slag [12] is one solution to this problem while manufacturing concrete or as a partial substitute for cement in the cement industry. High strength, better durability, avoidance of surface cracking of concrete, economic feasibility and sustainability are benefits of adding cementitious ingredients in concrete. The quantity of the cementitious material that replace OPC is limited by their pozzolanic activity [13].

Several researchers have reported that calcined kaolin (CK) called metakaolin can be used as a cementitious additive in concrete [14, 15]. The use of high reactivity CK as a supplemental cementitious ingredient in the concrete industry has gained popularity. Although CK has been known since the sixtieth of the last century. The studies are still interested in application of pozzolanic additives to cement as a cementitious material in concrete for improving its performance [16, 17]. CK is a very fine material fabricated by calcination of kaolinite clay at temperatures between 700 and 800 °C to remove chemically bonded water and disrupt the crystalline structure. CK refines the pore structure and reduces the lime hydroxide of the hardened matrix of the concrete. This is achieved as a result of the fine grained CK.

The reactions of CK with lime hydroxide produced during the hydration reactions of cement forming of secondary binding compounds such as calcium silicate hydrates (CSH) modifying the microstructure of concrete and contributing in improvement of the durability. The improvement can be confirmed by porosity, permeability, and chloride ion diffusivity [18]. CK particles are much smaller than cement particles but not finer than fumed silica [19]. Adding CK to concrete has a significant effect on the mechanical and durability characteristics [20, 21].

The use of calcined kaolinitic clay (CKC) derived from local quarries in south Sinai (low grade kaolin) reduces cement use which can assist to relieve environmental issues. Based on the above, the purpose of this study is to provide an overview of the use of the CKC in concrete. The qualities of CMK are first discussed, which mostly involve physical and chemical characteristics. After that, the hydration, workability, mechanical characteristics, durability and scan electron microscopy of CMC concrete are thoroughly investigated. Furthermore, the most relevant results and recommendations are offered, which will aid future concrete investigations using CKC. This material is also ecologically benign since it helps to reduce carbon oxides emissions into the atmosphere by lowering the amount of ordinary Portland cement (OPC) used [22]. CK can be used in place of ordinary Portland cement (OPC) in fabrication of concrete [23]. The relevant results and recommendations are reported, which will aid future concrete investigations.

2. Material and methods

2.1 CEM II 42.5R (EN 197-1)

Table 1 shows the physical properties OPC, while *Table 2* illustrates the chemical composition of OPC.

The properties	Value		Limits
Specific gravity	2.63		2.5 – 2.75
Bulk density, (kg/m³)	1780		-
The compressive strength for standard mortar (MPa)	2 days	20.8	Not less than 10
	28 days	50.3	Not less than 42.5
Soundness (La Chatelier)	1		Not more than 1
Setting time (min.)	Initial	135	Not less than 60
	Final	180	-

**ESS 4756-1/ 2013*

*Table 1 Mechanical and physical properties of OPC**
*1. táblázat A Portland cement (OPC) mechanikai és fizikai tulajdonságai**

Compound	SiO_2	Al_2O_3	Fe_2O_3	Cao	MgO	SO_3	Na_2O	K_2O	Cl^-	LOI
%	21.16	5.32	3.52	63.8	1.32	2.01	0.2	0.13	0.02	2.52

Table 2 Chemical composition of OPC
2. táblázat Az OPC kémiai összetétele

2.2 Calcined kaolinitic clay (CKC)

2.2.1 The chemical and mineralogical analysis of CKC

CKC was collected from aluminum Sulphate Company of Egypt. Kaolinitic clay (KC) was calcined in vertical fluidized bed kiln at 730 °C for 60 min [24]. The chemical composition based on the XRF was illustrated in *Table 3*. The amorphous silica is about 39% (*Fig. 1*). The XRD pattern displayed the silicate morphism in 20 – 25 2θ complying with that reported in reference [25, 26]. The chemical composition shows that the kaolinitic clay contains about 33% Al_2O_3, while the pure kaolinite contains 42% ($2SiO_2{\cdot}Al_2O_3{\cdot}2H_2O$), therefore KC contains 78.6% kaolinite.

Table 3 shows high content of reactive SiO_2; reactive silica represents the fraction of silica (39%) able to react at the normal conditions with alkalies forming binders. The averaged value of Al_2O_3 in CKC is 33%. CMK was analyzed by XRD analysis using a Bruker D8 Advanced Computerized X–Ray Diffractometer apparatus to show its constituting phases. *Fig. 1* displays that its main crystalline phase is quartz and the amorphous is metakaolin phase.

Compound	Amount (weight%)	
	CKC	CEM 1 42.5
SiO_2	61	21.5
SiO_2 (active)	39 = 0.65 Molar	-
Al_2O_3	33 = 0.32 M	3.5
SiO_2/Al_2O_3	2.3	-
Fe_2O_3	1.3	3.4
TiO_2	2.3	0.15
MgO	0.16	1.2
CaO	0.22	62
Na_2O	0.14	0.28
K_2O	0.13	0.32
SO_3	0.15	2.7
P_2O_5	0.10	0.04
SrO	0.05	-
Cl-	0.05	0.12
L.O.I	1.0	4.5
Total	99.6	99.71

Table 3 The chemical analysis of the calcined kaolinitic clay and CEM 1 42.5
3. táblázat A kalcinált kaolinites agyag és a CEM 1 42,5 kémiai elemzése

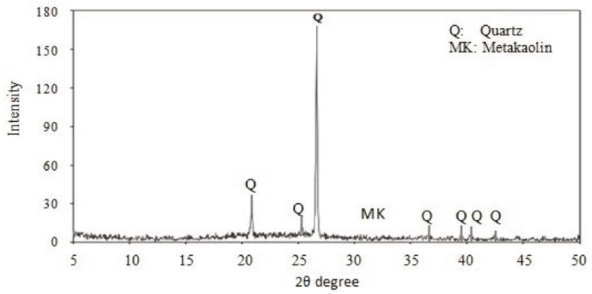

Fig. 1 XRD analysis for CKC
1. ábra Kalcinált kaolinitos agyag (CKC) XRD elemzése

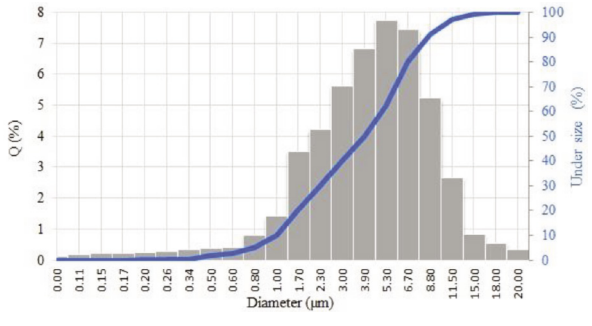

Fig. 2 Grain size distribution of the CKC by laser granulometry
2. ábra A CKC lézergranulometriával mért szemcseméret-eloszlása

2.2.2 The grain size-distribution of CKC

The grain size-distribution of CKC by laser granulometry was plotted in *Fig. 2* which shows that the diameter of CKC in cumulative 90% of below ~35 μm and 10% of below 4.5 μm with an average diameter of ~4.5 μm with a median at 50% = 4 μm and the mode (major) diameter = 5.5 μm.

2.2.3 The pozzolanic testing of calcined kaolinitic clay (CKC)

According to ASTM C 618 the pozzolanic materials reacts with portlandite [$Ca(OH)_2$] resulted from the hydration process of OPC and calcium silicate hydrate compound is formed as a cementing material. The pozzolanic reactivity of the samples was determined chemically by mixing of 2 g CKC with 10% lime and 2 drops of water. The free lime of the mixture was measured directly and after 5 days on another sample well covered and stored at 60 °C. This chemical method is described in detail elsewhere [27].

Table 4. indicates the pozzolanic activity, specific surface area and the bulk density of CKC. The reactivity test after 5 days recorded 120%.

The parameter	Value
The pozzolanic activity	120%
Specific surface area (BET)	20 m^2/g
The bulk density	1.35 g/cc

Table 4 The pozzolanic testing of calcined kaolinitic clay (CKC)
4. táblázat Kalcinált kaolinites agyag (CKC) puccolán vizsgálata

The surface area was measured by means of BET method which shows the adsorption of nitrogen at liquid nitrogen temperature. The specific density was evaluated using Le Chatelier flask according to ASTM C188-84. The mineralogical composition was monitored by means of X-ray diffraction using an automated diffract meter at a scan range from 10 to 50° (2θ). Positive reaction to pozzolana test (EN 196-4) was given by CKC when blended with CEM I 42.5R. Methylene blue method (UNI EN 933/9) 3.85 g/kg for CKC.

The replacement of OPC was made by addition of 5, 10, 15, 20, 25, 30 and 35% CKC in cement paste and the mortar mixes. The details of the mix proportions of the mortars are summarized in *Table 5*. The w/b ratio required to attain the standard consistency of the reference OPC paste was determined using Vicat apparatus according to ASTM C187-92. The initial and final setting times were measured using Vicat test according to ASTM C191-92. The same methods were utilized to investigate the effect of CKC on the water demand and the setting behavior of the pastes. The mixing procedures were carried out according to ISO 9597 (1989) and ASTM C305-82.

2.2.4 Differential thermal analysis (DTA) for Portland cement incorporating CKC

Fig. 3 shows DTA analysis of mixes containing a dosages of 0, 5, 10, 15, and 20% after 28 days of water curing. The main changes revealed by DTA analysis are as follows: An endothermic peak was detected before reaching 100 °C. This peak is related to the moisture absorbed by the sample from the environment. The endothermic peak observed in the 100-200 °C are attributed to the process of calcium silicate hydrate (CSH) formation. The peaks at the temperature range 450-500 °C are due to the dehydroxylation of $Ca(OH)_2$. The endotherms at the temperature near to 700 °C are due carbonation of lime and $CaCO_3$ (CC) formation. It is obvious that, as the cement replacement by CKC increases from 5% up to 15%, CSH content increases at the expense of lime hydroxide. Upon increasing the replacement dose to 20% CKC, insignificant variation in the C-S-H and CH content has recorded relatively to 15% CKC replacement. Increasing the replacement dose to 20% CKC, it seems that, the cementitious materials reactions between CKC and OPC were slowed down. These results are in agreement with previous research studies [28-30].

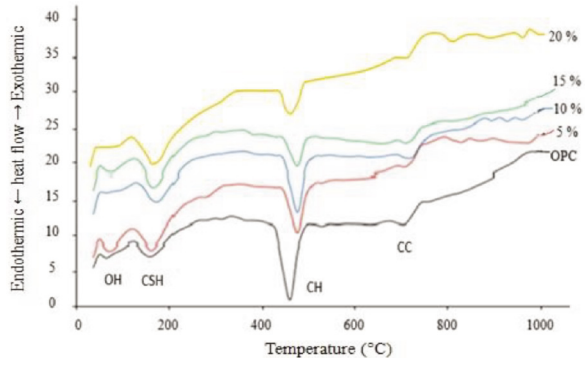

Fig. 3 Thermal properties analysis of CKC containing cement mixes (DTA)
3. ábra CKC tartalmú cementkeverékek (DTA) termikus tulajdonságainak vizsgálata

With replacement ratios of 0, 5, 10, 15 and 20% after 28 days of immersion in water.

2.2.5 Infrared spectrum analysis (FTIR)

This analysis was carried out to identify the structural state after replacement with CKC at 5, 10, 15 and 20% of cement and after 28 days of immersion in water. *Fig. 4* represents the infrared analysis of the reaction products with water after 28 days in the positive range 400-4000 cm^{-1}. There is a band at 3645 cm^{-1} due to the tension fluctuation of the OH group of portlandite $Ca(OH)_2$. The band at 1461 cm^{-1} is due to the presence of the mineral calcite (calcium carbonate) resulting from the interaction of lime with calcium dioxide. Band in the range 900 - 1000 cm^{-1} indicates the presence of a lattice structure of amorphous calcium silicate. The bands agree with that reported in references [31]. We notice from *Fig. 4* that the density of the band at 970 cm-1 in the aqueous mixtures of CKC/OPC increases with increasing the increase of CKC up to 15% of the cement. This behavior indicates an increase in the formation of aqueous calcium silicate compound. The density and pitch of the band begins to decrease with an increase in CKC of more than 15%. This is due to the decrease in pozzolanic reactivity.

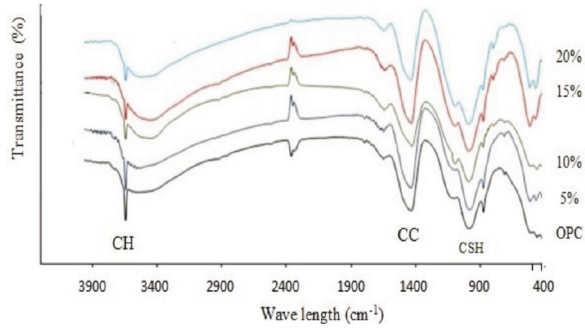

Fig. 4. FTIR analysis of cement mixes containing CKC with a replacement ratio of 0, 5, 10, 15, and 20% after 28 days of immersion in water
4. ábra 28 napos vízbe merítés után a 0, 5, 10, 15 és 20% CKC-t tartalmazó cementkeverékek FTIR elemzése

From the previous experiments conducted on (CKC/OPC) mixture, which contains increasing percentages of CKC, the manufactured product (5-20% CKC/OPC) and after 28 days of curing, to study the behavior of calcined kaolinitic clay as a pozzolanic material, using DTA /IR shows the following:

CKC behaves with cement as a pozzolanic material by interacting with calcium hydroxide resulting from the interaction of cement with water (Hydration) forming more calcium silicate hydrate binder (CSH). Therefore, this product behaves as pozzolanic materials according to the American standard specifications ASTM C618.

2.2.6 The fine aggregate

Using sand as a fine aggregate in both mortar and concrete mixtures. Sand tests were carried out according to the standard specifications (EN 1097, EN 933). The specific gravity = 2.6, the grain size averaged 2 mm.

2.2.7 Coarse aggregates

The chemical composition of coarse aggregates (dolomite) complying with Egyptian code No. 302/2018. The grain size averaged 16 mm.

2.2.8 The chemical additives

In order to achieve good mixing of the concrete mixtures, a water reducing agent, Master Reobuild 3045, was added, which conforms to ASTM 494 Type A.

3. Results and discussion

3.1 Cement mortar mixes

Eight mixtures of cement mortar were implemented using seven different replacement ratios with CKC from cement to test the compressive strength at the age of 7 days as an indicator of the pozzolanic activity of CKC, and based on the results obtained, the best substitution ratios were chosen to test them at the age of 28 days. *Table 5* shows the mixing ratios and the compressive strength resistance results for the different mixtures.

The basic mixing proportions of cement mortar were determined using ASTM C1240 standard, where the compressive strength of the mortar was measured at the age of 7 days using the average value of three cubes with dimensions of 50 x 50 x 50 mm using metakaolin substitution ratios of cement 5%, 10%, 15%, 20%, 25%, 30%, 35% and compared with the control mix that does not contain CKC.

The results of the compressive strength tests of the cement mortar showed that the substitution ratios (20%, 25%, 30%, 35%) achieved the best resistance ratios compared to the control mixture, ranging between 93% and 97.3%. *Fig. 5* shows the relative compressive strength of the mixtures containing CKC and the control mixture at the age of 7 days.

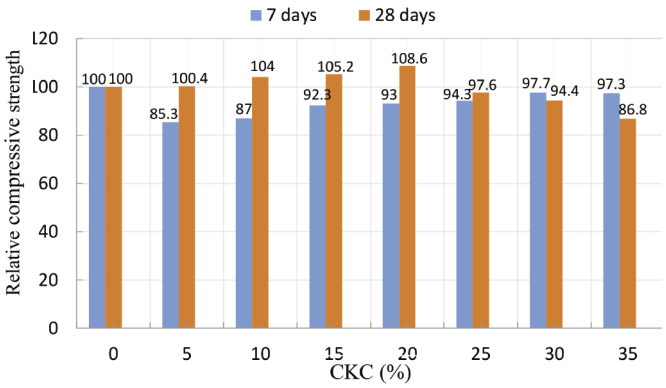

Fig. 5 Relative compressive strength of cement mortars at 7 and 28 days
5. ábra Cementhabarcsok 7 és 28 napos relatív nyomószilárdsága

Mixes	Cement (g)	CKC (g)	Sand (g)	Water (g)	Compressive strength	
					7 days (MPa)	28 days (MPa)
Control	500	–	1375	242	35 (100%)	50 (100%)
M-5	475	25	1375	242	30.2 (85.3%)	50.2 (100.4%)
M-10	450	50	1375	242	30.5 (87%)	52 (104%)
M-15	425	75	1375	242	32.3 (92.3%)	52.6 (105.2%)
M-20	400	100	1375	242	32.6 (93%)	54.3 (108.6%)
M-25	375	125	1375	242	33 (94.3%)	48.5 (97.6%)
M-30	350	150	1375	242	34.2 (97.7%)	47.2 (94.4%)
M-35	325	175	1375	242	33 (97.3%)	43.4 (86.8%)

Table 5 The mix proportions and compressive strengths
5. táblázat Keverési arányok és nyomószilárdságok

Mixes	Cement OPC	CKC	Fine aggregate	Coarse aggregate	Water	Chemical additive (liter)
Control	350	–	751	1126	168	6.2
C-5	332.5	17.5	751	1126	168	6.2
C-10	315	35	751	1126	168	6.2
C-15	297.5	52.5	751	1126	168	6.2
C-20	280	70	751	1126	168	6.2

Table 6 Ingredients of concrete mixes (kg/m³)
6. táblázat Betonkeverékek összetevői (kg/m³)

In the light of these results, the compressive strength of the four mixtures and the control mixture was measured at the age of 28 days using the average value of three molds with dimensions of 40 x 40 x 160 mm according to the standard specification EN196-1. *Fig. 11* shows that the replacement ratio of 20% of the cement with CKC is considered the best ratio, as the compressive strength was almost the same as the control mixture or slightly superior to it, while the replacement ratios of 25% and 30% gave lower values for the compressive strength reaching 94.4% and 97.7% respectively of the compressive strength of the control mix.

3.2 Concrete mixes

Based on the results of the pozzolanic tests and the compressive strength tests of cement mortar and on the economic consideration of the cost of concrete mixtures, the concrete mixtures were studied with replacement rates of cement with CKC 5%, 10%, 15%, 20% in the fresh state and the hardened state at the ages of 7, 28 and 90 days.

Table 6 shows the components of concrete mixtures per cubic meter. The mixtures were designed using the absolute volume method. The cement content of the control mix was 350 kg/m^3, the ratio of large to small aggregate (1:2.5). The ratio of water/cement materials (0.48) for all mixtures, chemical additives were used at a rate of 1.77 liters per 100 kg of cement materials. *Table 6* shows the results of concrete tests in its fresh and hardened states.

3.3 Concrete mixes tests

3.3.1 Slump test

The settling value of the mixtures was determined immediately after mixing according to ESS 1658. The results indicate that the slump values for the mixtures containing different percentages of CKC increased from the control mixture by a range of 20.6% to 26.3%.

3.3.2 Entrained air

The entrained air determination test was carried out according to ASTM C231. It is clear from *Table 7* that the content of air trapped in the mixtures that contain percentages of CKC was lower than in the control mixture by 6.5 to 21.7% with a replacement ratio of CKC of 5 to 15%.

3.3.3 Compressive strength

The compressive strength of the concrete was measured at the ages of 7, 28 and 90 days using the average value of three cubes with dimensions of 150×150×150 mm for each mixture at each age. The results showed that the early strength at the age of 7 days for the samples of the control mixture and the samples that contained 5% and 10% replacement rates achieved 80.5 and 80% respectively of the pressure resistance at the age of 28 days, while the samples that contained 15% and 20% replacement rates achieved 94.4% and 97.8% respectively of strength at the age of 28 days. Compared to the control mixture, the 5% ratio did not have a significant effect on the compressive strength at different ages. The use of 10% and 15% replacement ratios improved the strength by an average of 120.8 and 118.7% respectively at the age of 28 days.

At the age of 90 days, the results of the mixtures containing 15% replacement showed an improvement of 15% compared to the control mixtures. While the mixtures containing 20% substitution did not show any difference from the control mixtures.

4. Conclusions

In the light of the study of the properties of the local calcined kaolinitic clay using vertical kiln by fluidization CKC, it can be concluded that:

- CKC can be used as a replacement percentage of OPC cement.
- The optimal replacement ratios for cement with CKC 10% and 15%, which improved the compressive strength by an average of 120.8 and 118.7% at the age of 28 days, compared to the control mix.
- The use of CKC at replacement rates of 15% and 20% of the cement caused gaining of early strength at an age of 7 days of 94.4% and 97.8% of the strength of concrete at the age of 28 days.
- Based on the results of the preliminary stage of the study, the following can be recommended:
- Assessment of the optimal dosage out of the two ratios (10 & 15%) requires a study of their fulfillment of many characteristics as well as their effect on durability and sustainability and their efficiency in facing harmful elements and media. And then determine the best ratio from the technical and economic point of view.

Mixes	Slump (mm)	Air content (%)	Compressive strength (MPa) Concrete age (days)		
			7	28	90
Control	160	2.30	30.2	37.5	42.8
C-5	194 (+21.3%)	2.15 (- 6.5%)	31.0 (80.5% of 28 days)	38.5 (102.6%)	43.2 (100.9%)
C-10	198 (+23.8%)	1.90 (-17.4%)	36.3 (80.1% of 28 days	45.3 (120.8%)	46.3 (108.2%)
C-15	202 (+26.3%)	1.80 (-21.7%)	40.1 (94.4% of 28 days	44.5 (118.7%)	50.5 (118%)
C-20	193 (+20.6%)	2.00 (-13%)	40.3 (97.8% of 28 days	41.2 (109.9%)	45.3 (105.8%)

Table 7 Hardened concrete test results
7. táblázat A megszilárdult beton vizsgálati eredményei

References

[1] Smirnova, O.M.; Menéndez Pidal de Navascués, I.; Mikhailevskii, V.R.; Kolosov, O.I.; Skolota, N.S. (2021) Sound-Absorbing Composites with Rubber Crumb from Used Tires. Appl. Sci., 11, 7347. https://doi.org/10.3390/app11167347

[2] Alvee, A.R.; Malinda, R.; Akbar, A.M.; Ashar, R.D.; Rahmawati, C.; Alomayri, T.; Raza, A.; Shaikh, F.U.A. (2022) Experimental Study of the Mechanical Properties and Microstructure of Geopolymer Paste Containing Nano-Silica from Agricultural Waste and Crystalline Admixtures. Case Stud. Constr. Mater. (2021), 16, e00792. https://doi.org/10.1016/j.cscm.2021.e00792

[3] Althoey, F. Compressive Strength Reduction of Cement Pastes Exposed to Sodium Chloride Solutions: Secondary Ettringite Formation. Constr. Build. Mater. 2021, 299, 123965. https://doi.org/10.1016/j.conbuildmat.123965

[4] Marie, I.; Quiasrawi, H. Closed-Loop Recycling of Recycled Concrete Aggregates. J. Clean. Prod. 2012, 37, 243–248. https://doi.org/10.1016/j.jclepro.2012.07.020

[5] Ahmad, J.; Aslam, F.; Martinez-Garcia, R.; De-Prado-Gil, J.; Qaidi, S.M.A.; Brahmia, A.(2012) Effects of Waste Glass and Waste Marble on Mechanical and Durability Performance of Concrete. Sci. Rep., 11, 21525. https://doi.org/10.1038/s41598-021-00994-0

[6] Rahmawati, C.; Aprilia, S.; Saidi, T.; Aulia, T.B. (2021) Current Development of Geopolymer Cement with Nanosilica and Cellulose Nanocrystals. In Journal of Physics: Conference Series, Proceedings of the Annual Conference on Science and Technology Research (ACOSTER), Medan, Indonesia, 20–21 June 2021; IOP Publishing: Bristol, UK, pp. 1–8. https://doi.org/10.1088/1742-6596/1783/1/012056

[7] Ahmad, J.; Tufail, R.F.; Aslam, F.; Mosavi, A.; Alyousef, R.; Faisal Javed, M.; Zaid, O.; Khan Niazi, M.S. (2021) A Step towards Sustainable Self-Compacting Concrete by Using Partial Substitution of Wheat Straw Ash and Bentonite Clay Instead of Cement. Sustainability, 13, 824. https://doi.org/10.3390/su13020824

[8] Singh, M.; Choudhary, K.; Srivastava, A.; Sangwan, K.S.; Bhunia, D. (2017) A Study on Environmental and Economic Impacts of Using Waste Marble Powder in Concrete. J. Build. Eng., 13, 87–95. https://doi.org/10.1016/j.jobe.2017.07.009

[9] Taskin, A.; Fediuk, R.; Grebenyuk, I.; Elkin, O.; Kholodov, A. (2020) Effective Cement Binders on Fly and Slag Waste from Heat Power Industry of the Primorsky Krai, Russian Federation. Int. J. Sci. Technol. Res., 9, 3509–3512.

[10] Abdelgader, H.; Fediuk, R.; Kurpi´ nska, M.; Elkhatib, J.; Murali, G.; Baranov, A.V.; Timokhin, R.A. (2019) Mechanical Properties of Two-Stage Concrete Modified by Silica Fume. Mag. Civ. Eng., 89, 26–38. https://doi.org/10.18720/MCE.89.3

[11] Ahmad, J.; Martínez-García, R.; De-Prado-Gil, J.; Irshad, K.; El-Shorbagy, M.A.; Fediuk, R.; Vatin, N.I. (2022) Concrete with Partial Substitution of Waste Glass and Recycled Concrete Aggregate. Materials, 15, 430. https://doi.org/10.3390/ma15020430

[12] Dinakar, P.; Sethy, K.P.; Sahoo, U.C. (2013) Design of Self-Compacting Concrete with Ground Granulated Blast Furnace Slag. Mater., 43, 161–169. https://doi.org/10.1016/j.matdes.2012.06.049

[13] Sabir, B.B.; Wild, S.; Bai, J. (2001) Metakaolin and Calcined Clays as Pozzolans for Concrete: A Review. Cem. Concr. Compos., 23, 441–454. https://doi.org/10.1016/S0958-9465(00)00092-5

[14] Lee, G.; Ling, T.-C.; Wong, Y.-L.; Poon, C.-S. (2011) Effects of Crushed Glass Cullet Sizes, Casting Methods and Pozzolanic Materials on ASR of Concrete Blocks. Constr. Build. Mater., 25, 2611–2618.

[15] Vizcayno, C.; de Gutiérrez, R.M.; Castello, R.; Rodriguez, E.; Guerrero, C.E. (2010) Pozzolan Obtained by Mechanochemical and Thermal Treatments of Kaolin. Appl. Clay Sci., 49, 405–413. https://doi.org/10.1016/j.clay.2009.09.008

[16] Siddique, R.; Klaus, J. (2009) Influence of Metakaolin on the Properties of Mortar and Concrete: A Review. Appl. Clay Sci., 43, 392–400. https://doi.org/10.1016/j.clay.2008.11.007

[17] Güneyisi, E.; Geso˘ glu, M.; Karao˘ glu, S.; Mermerda¸s, K. (2012) Strength, Permeability and Shrinkage Cracking of Silica Fume and Metakaolin Concretes. Constr. Build. Mater., 34, 120–130. https://doi.org/10.1016/j.conbuildmat.2012.02.017

[18] Badogiannis, E.; Tsivilis, S. (2009) Exploitation of Poor Greek Kaolins: Durability of Metakaolin Concrete. Cem. Concr. Compos. 128–130. https://doi.org/10.1016/j.cemconcomp.2008.11.001

[19] Ding, J.-T.; Li, Z. (2002) Effects of Metakaolin and Silica Fume on Properties of Concrete. Mater. J., 99, 393–398.

[20] Bai, J.;Wild, S.; Sabir, B.B. (2002) Sorptivity and Strength of Air-Cured and Water-Cured PC–PFA–MK Concrete and the Influence of Binder Composition on Carbonation Depth. Cem. Concr. Res., 32, 1813–1821. https://doi.org/10.1016/S0008-8846(02)00872-4

[21] Güneyisi, E.; Mermerda¸ S, K. (2007) Comparative Study on Strength, Sorptivity, and Chloride Ingress Characteristics of Air-Cured and Water-Cured Concretes Modified with Metakaolin. Mater. Struct., 40, 1161–1171. https://doi.org/10.1617/s11527-007-9258-5

[22] Güneyisi, E.; Geso˘ glu, M.; Mermerda¸ S, K. (2008) Improving Strength, Drying Shrinkage, and Pore Structure of Concrete Using Metakaolin. Mater. Struct., 41, 937–949. https://doi.org/10.1617/s11527-007-9296-z

[23] Danish, P.; Ganesh, M.G. (2020) Behavior of Self-Compacting Concrete Using Different Mineral Powders Additions in Ternary Blends. Rev. Rom. Mater., 50, 232–239.

[24] Hoda S. Eldin, Nabil, A. Abdullah, Ismail Mahmoud F., Hashem Ahmed I. (2022) Preparation of meta phase of kaolinite as a precursor for geopolymer adsorbent fabrication Epitőanyag– Journal of Silicate Based and Composite Materials, Vol. 74, No. 3 (2022), 82–87. p. https://doi.org/10.14382/epitoanyag-jsbcm.2022.13.

[25] Ajayi, A.O., Atta, A.Y., Aderemi, B.O. and Adefila, S.S. (2010) Novel method of metakaolin dealumination -preliminary investigation" Journal of Applied Sciences Research, Vol. 6 No.10, 2010, pp. 1539-1541.

[26] Nabil A. Abdullah, El-Sokkary, T. M. – Gharieb, Mahmoud (2022): Synthesis of geopolymer binder from the partially de-aluminatedmetakaolinite by-product resulted from alum industry Epitőanyag– Journal of Silicate Based and Composite Materials, Vol. 74, No. 5 (2022), pp. 166–174. https://doi.org/10.14382/epitoanyag-jsbcm.2022.25.

[27] Javellana, M. P. and Jawed, I. (1982) Extraction of the free lime in Portland Cement and Clinker by Ethylene Glycol", Cement and Concrete Research, Vol. 12, 1982, pp. 309-403. Javellana, M. P. and Jawed, I. (1982) Extraction of the free lime in Portland Cement and Clinker by Ethylene Glycol", Cement and Concrete Research, Vol. 12, 1982, pp. 309-403. https://doi.org/10.1016/0008-8846(82)90088-6

[28] Palomo, A., Blanco-Varela, M.T., Granizo, M.L., Puertas, F., Vazquez, T., and Grutzeck, M.W., (1999) Chemical Stability of Cementitious Materials Based on Metakaolin", Cement and Concrete Research, Vol. 29, 1999, pp. 997. http://dx.doi.org/10.1016/S0008-8846(99)00074-5

[29] Mlinarik, L. and Kopecsko, K., (2013) Impact of Metakaolin – A New Supplementary Material- on the Hydration of Cements", ActaTechnica Napocensis: Civil Engineering & Architecture, Vol. 56, 2013, pp. 100.

[30] Juenger, M.C.G. and Siddique, R., (2015) Recent Advances in Understanding the Role of Supplementary Cementitious Materials in Concrete", Cement and Concrete Research, Vol. 78, 2015, pp. 71. https://doi.org/10.1016/j.cemconres.2015.03.018

[31] Trezza, M.A. and Lavat, A.E, (2001) Analysis of the System 2 CaO-Al2O3-CaSO4. 2H2O-CaCO3- H2O By FTIR Spectroscopy, Cem. Concr. Res., Vol. 31, 2001,pp. 869. https://doi.org/10.1016/S0008-8846(01)00502-6

Ref.:
Abdullah, Nabil A. – **Abdullah**, Hajer: *Calcined kaolinitic clay as a supplementary cementing material and its pozzolanic effect on concrete blends characteristics (Part I)*
Építőanyag – Journal of Silicate Based and Composite Materials, Vol. 75, No. 4 (2023), 142–147. p.
https://doi.org/10.14382/epitoanyag-jsbcm.2023.20

Ceramic nanocomposites: control of structural and PTX parameters of the synthesis of mullite from kaolinite using Taguchi experimental design

A. PONARYADOV ▪ Institute of Geology, FRC Komi Science Center of Ural Branch of RAS, Syktyvkar, Russia ▪ alex401@rambler.ru
O. KOTOVA ▪ Institute of Geology, FRC Komi Science Center of Ural Branch of RAS, Syktyvkar, Russia
E. KOTOVA ▪ St. Petersburg Mining University, St. Petersburg, Russia

Érkezett: 2023. 04. 25. ▪ Received: 25. 04. 2023. ▪ https://doi.org/10.14382/epitoanyag-jsbcm.2023.21

Abstract
The purpose of this article is to develop a special modeling approach, which simulates the synthesis of a mullite from kaolinite and allows controlling its physical and structural properties. A Taguchi experimental design is implemented to reveal significant PTX-parameters in comparison with insignificant ones for the synthesis of a mullite nanocomposite and prototyping of the optimal synthesis protocol.
The objects of the study are ceramic nanocomposites: morphostructural characteristics of mullite synthesized from kaolinite and its structural transformations during heat treatment. 2D contour plots of the intensity of mullite XRD-peaks and content of the mullite phase were used to visualize the influence of input factors and point out the optimal ones. Furthermore, we rearranged the previously proposed simple mathematical model of structural transformations "kaolinite – mullite", which allows controlling the synthesis protocol and properties of the mullite matrix of nanocomposite depending on the PTX-parameters of mullite synthesis.
Keywords: ceramic nanocomposites, mullite, kaolinite, Taguchi method, modeling, PTX-parameters
Kulcsszavak: kerámia nanokompozitok, mullit, kaolinit, Taguchi módszer, modellezés, PTX-paraméterek

Aleksei V. PONARYADOV
is a Researcher of Laboratory of Technology of Mineral Raw, Institute of Geology, Komi Science Center, Ural Branch of the Russian Academy of Sciences. Author and co-author of more than 30 scientific articles. Russian Mineralogical Society.

Olga B. KOTOVA
is professor and Head of Laboratory of Technology of Mineral Raw, Institute of Geology, FRC Komi Science Center, Ural Branch of the Russian Academy of Sciences. Author and co-author of 4 patents and more than 150 scientific articles.Vice-president of International Commission on Applied Mineralogy (IMA-ICAM). Member of Russian Mineralogical Society.

Elena L. KOTOVA
is a Scientific director of the Mining museum of the Saint-Petersburg Mining university. Author and co-author of chapter in book, 1 patent and 32 articles. The member of the Russian Mineralogical Society, Oil and gas historical Society of Russia.

1. Introduction

The synthesis of nanostructured natural-like functional materials based on natural mineral raw materials of various genesis seems to be a difficult task for technologists, which involves many necessary parameters within a unified multi-level system of the production process. The main disadvantage of natural raw materials is the presence of impurities affecting technological processes [1, 2] and quality of the target product [3-5]. Kaolin is known to be "the cleanest" clay from various "harmful" impurities for the production of ceramic nanocomposites. The use of these clays as a raw material is significantly reduced by the cost of production [6-8].

Mullite ceramics are multifunctional material, characterized by a high strength and a chemical stability in aggressive environments, which is widely used in various directions of industry, including high-temperature technological processes [9-11].

Mullite is formed from kaolin clay during heat treatment as a result of an exothermic reaction occurring in the interval of 1200–1400 °C (the solid-phase synthesis), which makes this process extremely energy-consuming [6, 12]. The temperatures at which the polymorphic transformations of the samples occur are explained by features of their chemical and phase compositions (including impurities [13, 14]), parameters of synthesis (heating rate [15]), structural features, for example, the presence of voids in mullite crystal lattice up to 0.067 nm leads to the formation of solid solutions with various oxides (Fe_2O_3, TiO_2, CaO, etc.), which also affects both technological properties of composites and synthesis protocol [16]. Thus, the synthesis of nanocomposites based on mineral raw materials of various genesis is a comprehensive task requiring the assessment of many parameters, which, within the framework of production, must be tied into a unified multi-level system.

Currently, the global trends and technological challenges, including the production of high-tech ceramics and nanocomposites, make the search for new approaches to assessing the purity and composition of raw materials [17, 18] and modeling the physicochemical properties of target prototypes for industrial applications [19-21] very relevant.

The use of mathematical approaches to calculating consistency of the relationship between the structure and properties of mineral raw materials for innovative environmentally friendly technologies for processing and operation, as well as to create ceramic composites with specified properties, can significantly reduce labor costs [22, 23]. In addition to the "classic" methods for calculating the kinetic constants of the reaction of the formation of mullite [24] and the assessment of thermodynamics of the process, mathematical modeling is used [25].

The mathematical modeling of mullite synthesis makes it possible to single out significant parameters in comparison with insignificant ones, simplifying the procedure for the synthesis of materials with specified characteristics. Design of experiments (e.g. Taguchi method, response surface methodology) is a powerful tool to simplify a huge number

of variables and minimize number of experiments for obtaining the optimum synthesis protocol. All parameters are systematically investigated as well as their interactions which made the acquired information more reasonable than results of influence of a separate factor. A key-feature of the Taguchi method is its versatility – applicability in various fields (electronics [26], biotechnology [27, 28], etc.) and a reduction in the number of experiments on finding optimal combination of parameters in the quality engineering [29, 30].

The aim of the study is to develop the near-to optimal synthesis protocol of a mullite nanocomposite from kaolinite with control of physical and structural properties of target product using Taguchi experimental design approach.

2. Methods and approaches

Solid-phase synthesis. Samples of kaolin clay (Vezhayu-Vorykvinsky deposit, Russia, the content of kaolinite >98%, the chemical composition is given in *Table 1*) were grinded in the laboratory disk grinder LDI-65. The load of 1.5–1.6 g was additionally grinded in the agate mortar and using the standard set of sieves was divided into fractions +0.1, –0.1+0.071, –0.071+0.05, –0.05 mm. As an introduced agent-crystallizer ("impurity"), mullite was used, which was previously synthesized according to the method [8], in the amount of 0.5, 1 and 5 wt.%. Heat treatment of samples and prepared mixtures with an agent-crystallizer was carried out at temperatures of 1100, 1150, 1200 °C in the atmosphere inside tube furnace Carbolite Gero TF1 16/60/300, heating rate 5, 10, 20 deg/min, holding time 2 hours at normal atmospheric pressure.

SiO_2	Al_2O_3	TiO_2	Fe_2O_3	K_2O	CaO	MgO
51.41	43.79	1.83	1.53	0.43	0.38	0.33

Table 1. Chemical composition of kaolin clay, wt.%
1. táblázat A kaolin agyag kémiai összetétele, tömegszázalékban

Calculation methods. The phase composition of the samples was determined by XRD-patterns of unoriented samples, X-ray diffractometer Shimadzu XRD-6000, radiation CuKα, Ni-filter, 30 kV, 20 mA, scanning range 2–65° 2θ. The phase content was evaluated by the Rietveld method (Profex software). Morphostructural characteristics of the samples were studied by scanning electron microscopy (SEM Axia ChemiSEM LoVac, Thermo Scientific).

To analyze the results of the experimental data and quality engineering of the resulting mullite nanocomposite, the Taguchi method was used, which is based on the use of Orthogonal Arrays (OA) [26]. As a target parameter, the intensity of mullite peaks on XRD-patterns was used.

To calculate the deviation between the experimental and optimal values of the input parameters, the Signal-to-Noise ratio (S/N) loss function was used. To optimize the synthesis protocol, the type of function "Higher-is-Better" (HB) was selected.

The values of the S/N ratio denoted by η_{ij}, where the i-th characteristic of the evaluated parameter obtained in the j-th experiment will be determined by the following logarithmic ratio:

$$\eta_{ij} = -10log\left(\frac{1}{n}\sum_{i=1}^{n} \frac{1}{I^2}\right) \quad (1)$$

where I stands for the resulting value (the intensity of the peak on the XRD-pattern), and n – the total number of experiments ran in the given experimental conditions.

The influence of experimental parameters ("weight") was determined by the Analysis of Variance (ANOVA) [29], by which instrumental errors in determining the intensities of mullite peaks on XRD-patterns are also evaluated.

3. Results and discussion

XRD, structural transformation of kaolinite. The crystalline structure of kaolinite includes alternating silicon tetrahedron and octahedral alumo-oxygen-hydroxyl layers [31, 32]. With an increase in temperature, as the interlayer water molecules are removed, there is a gradual decrease in the intensity of the reflections of X-ray radiation from the basal planes of kaolinite (peak at 2θ = 24.9°, green curve, *Fig. 1*). In the temperature range of 700–900 °C, the initial sample becomes almost X-ray amorphic (a significantly blurred area of diffuse scattering is preserved, which corresponds to the intermediate phase – metakaolinite). The mullite phase is fixed at temperatures above 1100 °C (peak at 2θ = 40.85°, red curve, *Fig. 1*). The crystalline structure of the mullite consists of paired Si_2O_5 chains, in which silicon ion is partially isomorphically substituted by aluminum ion, which has both the 6-fold [AlO_6] and the 4-fold [AlO_4] coordination [8, 33]. In parallel, cristobalite is formed due to an excess of unrelated silica (in mullite Al/Si = 3, while in the original kaolinite Al/Si = 2).

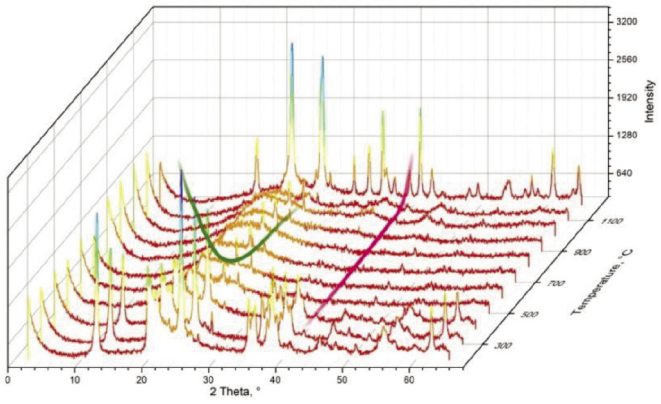

Fig. 1 Structural transformations of kaolinite during heat treatment
1. ábra Hőkezelés során a kaolinit szerkezeti átalakulásai

The morphostructural characteristics of the kaolinite and mullite synthesized at 1200 °C are represented in *Fig. 2*. The kaolin is most often represented by deformed and cemented individuals of kaolinite (*Fig. 2(a)*). Isometric crystals of kaolinite – hexagonal prisms – are rare. During heating, the matrix is recrystallized, which results in the formation of larger individuals of kaolinite. The sample heat treatment at temperatures above 1100 °C leads to the formation of elongated prismatic crystals of pseudomullite (*Fig. 2(b)*). The formation of new mineral phases begins on the surface and gradually spreads throughout the volume of the sample. At the last stages of temperature transformations, the appearance of cristobalite was recorded.

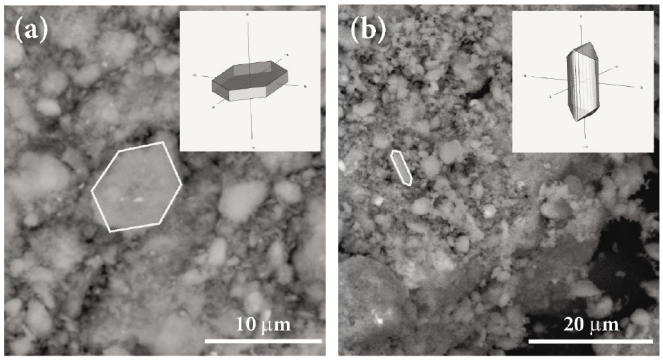

Fig. 2 Morphostructural characteristics of kaolinite (a) and mullite synthesized at 1200 °C (b) (SEM, back-scattered electrons)
2. ábra A kaolinit (a) és az 1200 °C-on szintetizált mullit (b) morfológiai jellemzői (SEM, visszaszórt elektronok)

It was shown [25], that for kaolinite, the intensity of peaks on XRD-patterns (*Fig. 1*) is approximated by linear dependence at temperatures below 450 °C and parabolic at higher temperatures, while for mullite the dependence is exponential: $I(t) = e^{(\pm I_0 \pm \alpha t)}$. The α-coefficient can be rearranged by introducing main parameters that affect the kinetics of the process of mullite synthesis – sample heating rate θ, concentration of the impurities σ, particles size d and k_i – proportionality coefficient, reflecting the "weight" of the influence of the considered parameters:

$$\alpha = \frac{k_1 \sigma}{k_2 \theta \cdot k_3 d} \quad (2)$$

Eq. (2) is a simplified mathematical model of structural transformations in the "kaolinite – mullite" series. However, the considering of the above mentioned synthesis input parameters one will need to run approximately one hundred experiments of mullite nanocomposite synthesis. To minimize number of experiments and clarify the interactions between the variables and obtain the optimum synthesis protocol the Taguchi method was used.

Parameter	1	2	3	4
***d*, particle size, mm**	–0.05	–0.071+0.05	–0.1+0.071	+0.1
***θ*, heating rate, deg/min**	5	10	20	–
***σ*, impurity concentration, wt. %**	0	0.5	1	5
***t*, holding temperature, °C**	1100	1150	1200	–

Table 2 Design parameters of mullite synthesis
2. táblázat A mullit szintézisének tervezési paraméterei

Parameter	1	2	3	4
d	50.52	47.89	54.71	51.80
θ	53.63	51.05	52.92	–
σ	51.91	51.55	50.74	50.16
t	44.43	55.34	54.87	–

Table 3 Average values η
3. táblázat Átlagértékek η

The mullite was synthesized at normal pressure varying such input parameters as particle size, heating rate, holding temperature and impurities concentration (which will correspond to the orthogonal array $4^2 \times 3^2 = 144$). The parameters values are presented in *Table 2*, η average values calculated by the ANOVA method – in *Table 3*.

Fig. 3 shows $S/N=\eta$ deviation from its average value. The results of the application of the ANOVA method for data processing are given in *Table 4*.

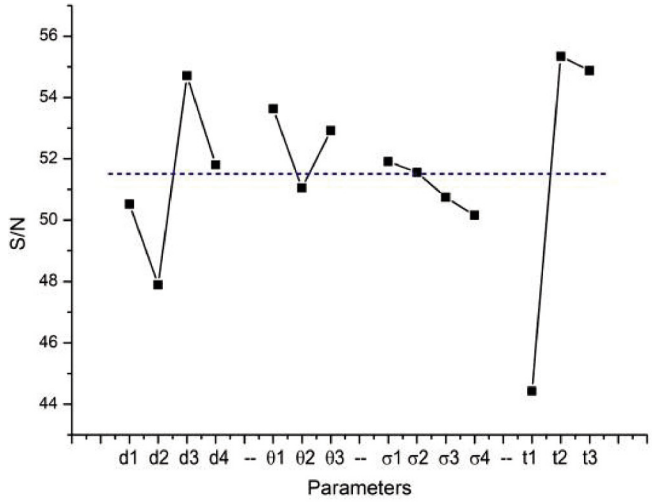

Fig. 3 S/N=η deviation from average value (dashed line)
3. ábra S/N=η eltérés az átlagértéktől (szaggatott vonal)

Parameter	Number of degrees of freedom (df_p)	Sum of squares SS_p	Variance, V	Fisher's criterion F	Parameter influence (%)
d	3	74.45	24.82	0.67	6.48
θ	2	23.90	11.95	0.32	3.12
σ	3	10.13	3.38	0.09	0.88
t	2	685.15	342.58	9.26	89.51
Error	27	296.03	37.00		

Table 4 ANOVA results
4. táblázat ANOVA eredmények

Size of the particles. Reducing the size of the particles results in decreasing temperature of structural transformations (also due to the intensification of diffusion processes during the reaction). Platova and co-authors [34] showed, that in addition to large energy expenses during fragmentation, the regrinding can result in undesirable aggregation of kaolinite particles and, accordingly, to a decrease in the reactionary ability of the surface.

Heating rate. A more uniform heating of the sample, which begins on the surface and gradually spreads throughout the volume of the kaolinite particles, can be achieved with reducing the rate of heat supply (heating rate).

Influence of impurities. The positive impact of impurities is associated with their ability to intensify the process of crystallization-pseudocoagulation structure by accelerating the reaction (for example, with the introduction of group II cations), increasing of mullite yield (TiO_2, LiCl, $MgCO_3$, LiF, etc.) or creating additional crystallization centers (for example, introducing 0.1–1% of the filamentous mullite stimulates crystal formation) [35, 36]. We used impurities of mullite particles as additional crystallization centers.

The formation of the target product – a mullite nanocomposite – has a number of intermediate phases (metakaolinite, pseudomullite) [8]:

$$3(A1_2O_3 \cdot 2SiO_2 \cdot 2H_2O) \Rightarrow 3A1_2O_3 \cdot 2SiO_2 + 4SiO_2 + 6H_2O \quad (3)$$
kaolinite *mullite* *cristobalite*

The theoretical ratio of phases of mullite and cristobalite formed as a result of this reaction is 63.9% to 36.1%. Loss of this ratio indicates the incompleteness of the crystalline transformation of kaolinite with the formation of only intermediate spinel-like phase and pseudomullite, which cannot be reliably identified using X-ray phase analysis.

The influence of input factors – particle size and heating rate – on the intensity of the XRD-peaks of mullite is visualized on the 2D contour plots (*Fig. 4(a)*). *Fig. 4(b)* shows dependence of the content of the mullite phase in the samples on the size of the particles and the heating rate. A comparison of the above contour plots shows that the areas of the greatest intensity of the peaks of the mullite (red region, *Fig. 4(a)*) and the content of the mullite phase in the synthesized sample closest to the theoretical value (blue area, *Fig. 4(b)*) practically coincide. The optimal result is achieved with the size of the particles –0.071+0.1 mm and heating rate 12 deg/min.

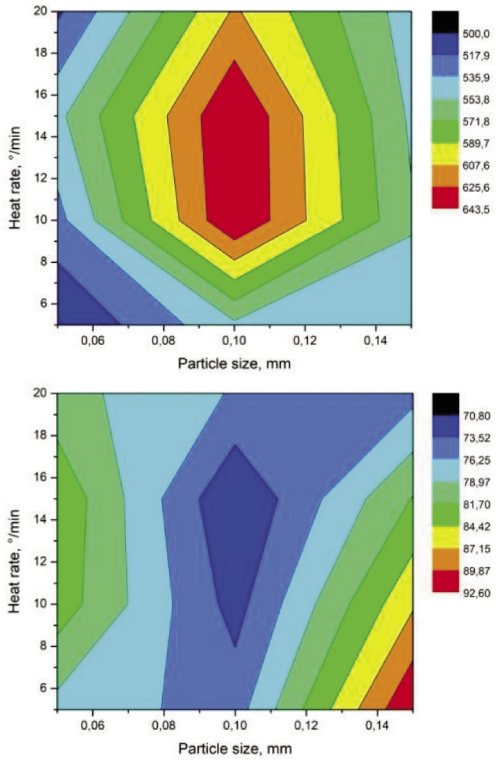

Fig. 4 *2D contour plots of the dependence of the intensity of mullite peaks (a) and content of the mullite phase (b) on the size of the particles and the heating rate. Holding temperature 1150 °C*

4. ábra *2D kontúrdiagramok a mullitcsúcsok intenzitásának (a) és a mullitfázis tartalmának (b) függéséről a részecskék méretétől és a fűtési sebességtől. Tartási hőmérséklet 1150 °C*

The synthesis of mullite nanocomposite from kaolinite in the framework of the optimal protocol was tested (the impurities concentration was 0.5 wt.% corresponding to the point in *Fig. 3*, which is the closest to the average value η). The obtained values of the intensity of the mullite peak (at $2\theta = 40.85°$) at different holding temperatures lie higher than the values measured earlier (the size of the particles +0.1 mm and the heating rate of 10 deg/min, without the introduction of additional crystallization centers), which confirms the formation of the mullite phase at lower temperatures (*Fig. 5*). Taking into account the calculated values (*Table 4*), the proportionality coefficients were calculated: $k_1 = 1.756$, $k_2 = 6.226$, $k_3 = 12.931$.

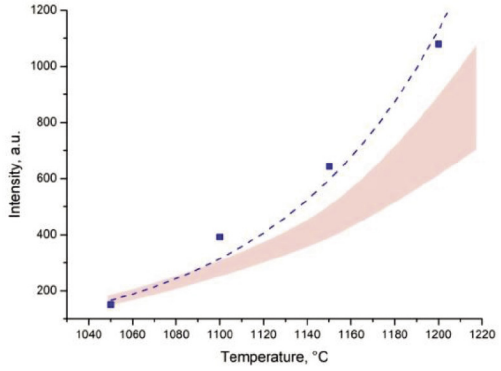

Fig. 5 *Dependence of the intensity of mullite peaks on the temperature of the experiment (dashed curve) with particle sizes –0.071+0.1 mm and a heating rate 12 deg/min. The pink area – values of intensity of mullite peaks in the initial experiments (see Table 2)*

5. ábra *A mullitcsúcsok intenzitásának függése a kísérlet hőmérsékletétől (szaggatott görbe) -0,071+0,1 mm-es részecskeméret és 12 fok/perc fűtési sebesség mellett. A rózsaszín terület - a mullitcsúcsok intenzitásának értékei a kezdeti kísérletekben (lásd a 2. táblázatot)*

The analysis of SEM images confirmed that the optimal protocol is achieved with the sizes of the initial kaolinite particles –0.071+0.05 and –0.1+0.071 mm and temperatures 1150 and 1200 °C, which is consistent with the result obtained above using the Taguchi method and analysis of variance (ANOVA).

Fig. 6 shows the change in the structure of the material under study during heat treatment, depending on the particle size. As the treatment temperature increases, kaolinite grains recrystallize to form larger subindividuals. In addition, elongated pseudomullite crystals appear. At temperatures of 1150 and 1200 °C, the main volume of the samples is compacted; also, at these temperatures, the formation of secondary mullite is typical. It should be noted that –0.05 mm kaolinite fraction is characterized by the formation of subaggregates at lower temperatures than larger fractions. This results in inhibition of the processes of structural transformation of the test substance.

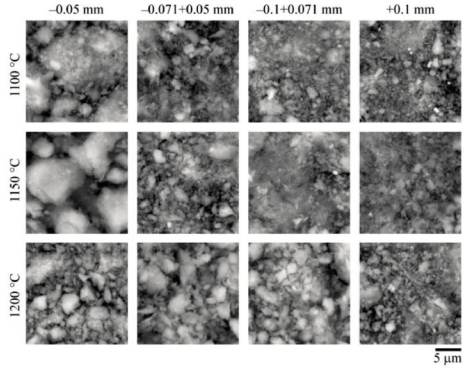

Fig. 6 *Changes in the structure of kaolinite samples with a change in the holding temperature (SEM, back-scattered electrons)*

6. ábra *A kaolinitminták szerkezetének változása a hőmérséklet változásával (SEM, visszaszórt elektronok)*

4. Conclusion

A numerical modeling approach for engineering the quality of a mullite nanocomposite, its physical and structural properties and an optimal synthesis protocol were realized.

Implementing Taguchi experimental design method and analysis of variance (ANOVA) we marked significant parameters in comparison to insignificant ones to obtain nanocomposites with specified characteristics of the ceramic matrix and create the optimal synthesis protocol. On the basis of the obtained experimental data, a mathematical model was re-calculated taking into account the structural and PTX-parameters of the synthesis of mullite from kaolinite.

The 2D contour plots of the intensity of mullite XRD-peaks and content of the mullite phase (mullite content in the synthesized nanocomposite) on the particle size and heating rate showed that the optimal synthesis protocol will be achieved at a particle size of –0.071+0.1 mm and a heating rate of 12 deg/min, which was also confirmed by the experiments. The –0.05 mm fraction of the studied kaolinite was characterized by a higher degree of recrystallization than larger fractions. This resulted in the formation of large subaggregates of kaolinite and, accordingly, to the inhibition of the processes of structural transformation and the formation of the mullite phase.

This paper is a contribution to the development of a technology strategy (process-properties-optimization) for the producing of a mullite nanocomposite with specified technical properties based on structural transformations in the "kaolinite - mullite".

5. Acknowledgements

The work was conducted partly within the framework of the research task [number 1021051101666-2-1.5.1; FUUUU-2022-0059] to develop a technique for estimating the content of aluminosilicate phases on the example of mullite, partly within the framework of RSF project [number 21-47-00019]: study of stability of physicochemical constitution and morphostructural characteristics of mullite.

References

[1] Chakraborty, A.K. (2014) Phase Transformation of Kaolinite Clay. Springer New Delhi. 342 p. http://dx.doi.org/10.1007/978-81-322-1154-9

[2] Cui, K., Zhang, Y., Fu, T. et al. (2020) Toughening Mechanism of Mullite Matrix Composites: A Review. THE Coatings. Vol. 10, pp. 672-696. http://dx.doi.org/10.3390/coatings10070672

[3] Li, S., Li, N. (2005) Influences of composition of starting powders and sintering temperature on the pore size distribution of porous corundum-mullite ceramics. Science of Sintering. Vol. 37, No. 3, pp. 173-180. http://dx.doi.org/10.2298/SOS0503173S

[4] Al-Shantir, O., Trník, A., Csáki, Š. Influence of firing temperature and compacting pressure on density and Young's modulus of electroporcelain. (2018) AIP Conference Proceedings. Vol. 1988, 020001. http://dx.doi.org/10.1063/1.5047595

[5] De Aza, A.H., Turrillas, X., Rodriguez, M.A. et al. (2014) Time-resolved powder neutron diffraction study of the phase transformation sequence of kaolinite to mullite. Journal of the European Ceramic Society. Vol. 34, No. 5, pp. 1409-1421. http://dx.doi.org/10.1016/j.jeurceramsoc.2013.10.034

[6] Egorova, E.Y., Vakalova, T.V., Pogrebenkov, V.M. (2006) Porous ceramics for catalyst carriers based on natural aluminosilicate raw materials. Refractories and technical ceramics. Vol. 7, pp. 30 – 37.

[7] Kacher, E.B., Kremnev, D.V., Mishchenko, A.V. et al. (2006) Research and optimization of the composition and conditions for the synthesis of ceramic products. Scientific and technical bulletin of information technologies, mechanics and optics. Vol. 26, pp. 373-377.

[8] Kotova, O.B., Ustyugov, V.A., Sun, S., et al. (2022) Mullite production: phase transformations of kaolinite, thermodynamics of the process. Journal of Mining Institute. Vol. 254, pp. 129-135. http://dx.doi.org/10.31897/PMI.2022.43

[9] Abdullayev, A., Avcioglu, C., Fey, T., et al. (2022) Fabrication and characterization of porous mullite ceramics derived from fluoride-assisted Metakaolin-Al(OH)3 annealing for filtration applications. Open Ceramics. Vol. 9, 100240. http://dx.doi.org/10.1016/j.oceram.2022.100240.

[10] Romero, M., Padilla, I., Contreras, M., et al. (2021) Mullite-Based Ceramics from Mining Waste: A Review. Minerals. Vol. 11, No. 3, pp. 332. https://doi.org/10.3390/min11030332

[11] Vakalova, T.V., Devyashina, L.P., Tokareva, A.Y. (2013) New mineralizing additive for solid-phase synthesis of mullite and sintering of mullite ceramics from oxides. New refractories. Vol. 3, p. 63.

[12] Pavlov, V.F. (1977) Physical and chemical bases of firing of building ceramics. Stroyizdat, Moscow, 240 p.

[13] Yuan, L., Zhenli, L., Yan, Z., et al. (2022) Effect of mullite phase formed in situ on pore structure and properties of high-purity mullite fibrous ceramics. Ceramics International. Vol. 48, No. 3, pp. 3578-3584. https://doi.org/10.1016/j.ceramint.2021.10.136.

[14] Pletnev, P.M., Pogrebenkov, V.M., Vvereshchagin, V.I., et al. (2017) Mullite-corundum materials based on mullite binder, resistant to high-temperature deformations. New refractories. Vol. 11, pp. 36-43.

[15] Teklay, A., Yina, C., Rosendahl, L., et al. (2015) Experimental and modeling study of flash calcination of kaolinite rich clay particles in a gas suspension calciner. Applied Clay Science. Vol. 103, pp. 10–19. https://doi.org/10.1016/j.clay.2014.11.003

[16] Vakalova, T.V., Pogrebenkov, V.M., Shlyaeva, N.P. (2009) Influence of structural and mineralogical features of silica raw materials on phase changes during its heating. New refractories. Vol. 1, pp. 18-22.

[17] Kotova, O.B., Ignatiev, G.V., Shushkov, D.A. et al. (2019) Preparation and Properties of Ceramic Materials from Coal Fly Ash. Minerals: Structure, Properties, Methods of Investigation Springer. Proceedings in Earth and Environmental Sciences. Springer, Cham. P. 100-107. https://doi.org/10.1007/978-3-030-00925-0_16

[18] Tong, L.X., Li, J.H., Liu, F. (2012) Preparation of Mullite Nanocomposites Powders by the Hydrothermal Crystallization Method from Coal Gangue. Key Engineering Materials. Vol. 512-515, pp. 49-53. https://doi.org/10.4028/www.scientific.net/KEM.512-515.49

[19] Alfonso, P., Penedo, L., Garcia-Valles, M., et al. (2022) Thermal behavior of kaolinitic raw materials from San José (Oruro, Bolivia). Journal of Thermal Analysis and Calorimetry. Vol. 147, pp. 5413–5421. https://doi.org/10.1007/s10973-022-11245-3

[20] Iyasara, A., Boston, R.H., Schmidt, W., et al. (2016) Protocols for the Fabrication, Characterization, and Optimization of n-Type Thermoelectric Ceramic Oxides. Chemistry of Materials. Vol. 29, No. 1, pp. 265–280. https://doi.org/10.1021/acs.chemmater.6b03600

[21] Romero, A.R., Elsayed, H., Bernardo, E. (2018) Highly porous mullite ceramics from engineered alkali activated suspensions // Journal of the American Ceramic Society. Vol. 101, pp. 1036-1041. https://doi.org/10.1111/JACE.15327

[22] Shaneva, A.S., Popova, N.A., Koltsova, E.M. (2017) Research and mathematical modeling of the process of obtaining a ceramic composite material SiC-CNT. Advances in Chemistry and Chemical Technology. Vol. 31, No. 8, pp. 42-44.

[23] Marukovich, E.I., Nikolaychik, Y.A. Improving the efficiency of mold coatings by modifying with nanostructured materials: [non-stick coatings]. (2018) Actual problems of strength: monograph [based on the materials of the 60th International scientific conference "Actual problems of strength", 14–18, May, 2018, Vitebsk] : in 2 volumes / National Academy of Sciences of Belarus, Vitebsk State Technological University. edited by V. V. Rubanik. Vitebsk: VSTU. Vol. 2, Ch. 12, pp. 231-253.

[24] Kosenko, N.F., Filatova, N.V., Pimkov, Y.V. Kinetics of Solid-Phase Synthesis of Mullite from Activated Precursors. (2016) Izvestia of Higher

Educational Institutions. Chemistry and chemical technology. Vol. 59, No. 1, pp. 36-38.
[25] Ponaryadov, A.V., Ustyugov, V.A., Kotova, E.L. (2022) Mathematical approach to studying the process of mullite synthesis. Vestnik of geosciences. Vol. 335, No. 11, pp. 48-54. https://doi.org/10.19110/geov.2022.11.6
[26] Hüner, E. (2020) Optimization of axial flux permanent magnet generator by Taguchi experimental method. Bulletin of the Polish Academy of Sciences, Technical Sciences. Vol. 68, No. 3, 133378
[27] Kokcam, A.H., Uygun, Ö., Taskin, M.F., et al. (2018) Modelling Porosity Permeability of Ceramic Tiles using Fuzzy Taguchi Method. Open Chemistry. Vol. 16, No. 1, pp. 1111-1114. https://doi.org/10.1515/chem-2018-0117
[28] Danilkovich, A.V., Turobov, V.I., Sobolev, E.V., et al. (2016) Application of the Taguchi method to study the structure of a peptide ligand in a complex complex. Mathematical Biology and Bioinformatics. Vol. 11, No. 2, pp. 385–393. https://doi.org/10.17537/2016.11.3851
[29] Celik, N., Turgut, E. (2012) Design analysis of an experimental jet impingement study by using Taguchi method. Heat and Mass Transfer. Vol. 48, pp. 1407-1413. https://doi.org/10.1007/S00231-012-0989-7
[30] Chen, H.J., Chang, S.N., Tang, C.W. (2017) Application of the Taguchi Method for Optimizing the Process Parameters of Producing Lightweight Aggregates by Incorporating Tile Grinding Sludge with Reservoir Sediments. Materials. Vol. 10, No. 11, 1294. https://doi.org/10.3390/ma10111294
[31] Bortnikov, N.S., Mineeva, R.M., Novikov, V.N., et al. (2011) Influence of the size effect on the crystal-morphological properties of kaolinite according to electron microscopy and EPR data (Zhuravliny Log deposit, South Urals). Reports of the Russian Academy Sciences. Vol. 439, No. 2, pp. 240-243.
[32] Shehu, Y., Suzi, S.J., Nur Azam, B. et al. (2017) Chemical Composition and Particle Size Analysis of Kaolin. Path of Science. Vol. 3, No. 10, pp. 1001-1004. https://doi.org/10.22178/pos.27-1
[33] Menezes, R.R., Farias, F.F., Oliveira, M.F., et al. (2009) Kaolin processing waste applied in the manufacturing of ceramic tiles and mullite bodies. Waste Management & Research. Vol. 27, No. 1, pp. 78-86. https://doi.org/10.1177/0734242X07085338
[34] Platova, R.A., Argynbaev, T.M., Stafeeva, Z.V. (2012) Influence of dispersity of kaolin from the Zhurnavliny Log deposit on the pozzolanic activity of metakaolin. Building materials. Vol. 2, pp. 75-79.
[35] Yarotskaya, E.G., Fedorov, P.P. (2018) Mullite and its isomorphic substitutions: review. Condensed media and interfaces. Vol. 20, pp. 537-544. https://doi.org/10.17308/kcmf.2018.20/626
[36] Roy, J., Maitra, S. (2015) Mullitization of aluminosilicate diphasic gel in the presence of nickel oxide additive. Journal of Composite Materials. Vol. 49, No. 13, pp. 1579-1588. https://doi.org/10.1177/0021998314536071

Ref.:
Ponaryadov, A. – **Kotova**, O. – **Kotova**, E.: *Ceramic nanocomposites: control of structural and PTX parameters of the synthesis of mullite from kaolinite using Taguchi experimental design*
Építőanyag – Journal of Silicate Based and Composite Materials, Vol. 75, No. 4 (2023), 148–153. p.
https://doi.org/10.14382/epitoanyag-jsbcm.2023.21

Systematic Review of Natural Rubber Latex Modified Concrete for Eco efficient Construction Works

Efiok Etim NYAH ▪ Department of Civil Engineering, University of Cross River State, Nigeria
David Ogbonna ONWUKA ▪ Department of Civil Engineering, Federal University of Technology Owerri, Imo State, Nigeria
George Uwadiegwu ALANEME ▪ Department of Civil Engineering, Kampala International University, Kampala, Uganda ▪ alanemeg@kiu.ac.ug
Ulari Sylvia ONWUKA ▪ Department of Project Management, Federal University of Technology Owerri, Imo State, Nigeria

Érkezett: 2023. 07. 28. ▪ Received: 28. 07. 2023. ▪ https://doi.org/10.14382/epitoanyag-jsbcm.2023.22

Abstract

The paper presents a systematic review of the literatures on natural rubber latex modified concrete (NRLMC) which is a composite material that combines the benefits of both natural rubber latex (NRL) and concrete. The use of NRL in concrete mixtures can improve its workability, durability and microstructural properties and the concrete exhibits excellent mechanical properties such as high tensile and flexural strength, impact resistance and energy absorption capacity. Additionally, NRLMC can reduce the carbon footprint of the construction industry by incorporating NRL to substitute the quantity of cement in the concrete mix. The performance of NRLMC is influenced by various factors such as the type and dosage of NRL, curing conditions and mixing methods. This paper provides a review of the existing literatures on the use RLMC, including its properties, limitations and challenges, and also highlights its potentials by addressing sustainability and environmental concerns. Moreover, the review study of soft computing tool deployment such as adaptive neuro-fuzzy inference system (ANFIS) in the evaluation of NRLMC engineering properties was carried out in this research. The findings of this paper can guide the optimization of NRLMC for various applications and facilitate the adoption of this innovative material in the construction industry, also, the use of ANFIS can reduce the need for costly and time-consuming experimental testing, making the development of NRLMC more efficient and cost effective.

Keywords: Natural rubber latex, Ecofriendly concrete, Neuro fuzzy, artificial intelligence
Kulcsszavak: Természetes gumilatex, környezetbarát beton, Neuro fuzzy, mesterséges intelligencia

Efiok E. NYAH
is a lecturer in the Department of Civil Engineering, University of Cross River State, Nigeria. He specializes in civil and structural engineering. He is a member of the Nigerian Society of Engineers and a registered engineer with the Council for the Regulation of Engineering in Nigeria. He is interested in analytical, computational, and experimental research, including field and laboratory testing methods on sustainable and eco-friendly materials for civil engineering works and structures.

David O. ONWUKA
is a Professor in the Department of Civil Engineering, Federal University of Technology, Owerri. His research interest include structural dynamics, structural materials and modeling. He is a member of several learned and professional societies.

George U. ALANEME
is an Assistant Lecturer in the department of Civil Engineering at Kampala International University, Kampala with a good command of the required software programs used in automated design, analysis, and optimization. He has extensive experience in the design of linear, nonlinear, and discrete optimization problems as well as working knowledge of algorithm development and its application to solving civil engineering problems. He's a registered engineer under the Council for Regulation of Engineers in Nigeria (COREN).

Ulari S. ONWUKA
is a lecturer in the Department of Project Management, Federal University of Technology, Owerri. She is interested in building materials, construction technology and project management. She belongs to several professional bodies.

1. Introduction

In the construction industry, there is growing interest in utilizing locally available and renewable resources to produce environmentally friendly and energy-efficient cement concrete. Natural rubber latex (NRL) is a natural polymer obtained from renewable sources, offering the potential for sustainable construction practices by effectively modifying cement composites [1]. NRL can be employed to modify cement composites, particularly concrete. Derived from the Hevea brasiliensis tree through a natural polymerization process, NRL is a milky white liquid consisting of a complex mixture of proteins, carbohydrates, and lipids [2, 3].

Incorporating NRL into concrete mixtures leads to the production of NRLMC, which can benefit from the unique properties of NRL. This approach promotes the use of renewable resources and supports sustainable construction practices [4]. The incorporation of NRL in concrete enhances workability by reducing water demand and increasing cohesion. Its long polymer chain structure improves binding properties, adhesion, and mechanical strength by forming a network of bonds [5]. NRL also contributes to a denser microstructure by creating a latex film that fills voids and microcracks, making the concrete impermeable. This improves durability by protecting against chemical attacks, freeze-thaw cycles, and water penetration [6, 7]. NRL modified concrete performs better in aggressive environments like marine areas, sewage plants, and acidic conditions compared to regular concrete [8]. However, it is important to consider the elastomeric effect and compositional stability of NRL at elevated temperatures, and coagulation can be mitigated by adding substances like ammonia-tetramethyl thiuram di-sulfide or zinc oxide. These considerations ensure the effective utilization of NRL in concrete applications [9].

Fig. 1 Natural Rubber Latex [5]
1. ábra Természetes gumi latex [5]

In addition, the use of NRL in the concrete mix can help to reduce the risk of segregation and bleeding, which are

common problems in traditional concrete mixes. Segregation occurs when the aggregates in the concrete mix separate from the cement paste, resulting in a non-uniform mix that can weaken the final product. Bleeding occurs when water rises to the surface of the concrete and forms a layer of water on top, which can weaken the surface and reduce the durability of the concrete [10]. The addition of NRL can help to reduce these problems by improving the cohesion of the mix and reducing the water demand. Overall, NRLMC can offer improved workability compared to traditional concrete, which can make it a more attractive option for construction projects. The improved workability can result in a concrete that is easier to handle, place, and finish, with improved surface finish and appearance [11].

Polymer latex is commonly used in cementitious materials to enhance properties like durability, adhesion, mechanical strength, toughness, and crack resistance [12]. There is a growing interest in utilizing locally available and renewable resources, such as Natural Rubber Latex (NRL), to improve the mechanical strength and durability of concrete [13, 14]. NRL is a natural, renewable resource obtained from the Hevea Brasiliensis tree through a natural polymerization process. It mainly consists of cis-1,4-polyisoprene (94% hydrocarbon) along with non-rubber constituents (6%) and various mineral components like K, Na, Mg, Ca, Cu, and Fe [15, 16]. Studies have investigated the effects of incorporating NRL into cement mortar and high-performance concrete. Optimal proportions of NRL were determined to achieve waterproof concrete and enhance thermal insulation [17, 18]. Additionally, NRL was found to improve the durability of steel fiber-reinforced concrete, with a decrease in chloride ion permeability observed when NRL was added at a proportion of 0.5% by weight of cement. These findings demonstrate the potential of NRL as an effective additive for enhancing the properties and durability of concrete [19].

Artificial intelligence (AI) refers to the simulation of human intelligence in machines that are programmed to think and learn like humans. AI technologies enable machines to learn from experience, adjust to new inputs, and perform tasks that typically require human intelligence, such as visual perception, speech recognition, decision-making, and language translation [20, 21]. The potential benefits of AI include increased efficiency, improved decision-making, and enhanced quality of life. However, there are also concerns about the potential risks and ethical implications of AI, such as job displacement, bias, and privacy violations [22]. AI tool such as neuro-fuzzy hybrid smart intelligent models have the potential to revolutionize many industries, including civil engineering and building construction. One area where AI can be applied is in the development and use of NRLMC [23]. Overall, the application of AI in NRLMC has the potential to improve the durability and cost-effectiveness of this innovative construction material, making it more widely adopted in the industry [24]. AI techniques can be adapted in various ways to optimize the production and use of NRLMC such as;

i. Predictive modeling: AI with supervised learning algorithm such as adaptive neuro fuzzy inference system can be used to develop predictive models that can accurately estimate the strength and durability of NRLMC based on its mix design and environmental conditions. This can help engineers, project managers and architects to optimize the mix design of concrete and reduce the amount of trial-and-error required in the development process and also material wastage [25].
ii. Quality control: AI can be used to monitor the quality of NRLMC during production and construction. By analyzing real-time data from sensors and cameras, AI can detect defects and anomalies, such as cracks or air pockets, and alert workers to take corrective actions in order to optimize the quality of the final product [26].
iii. Material optimization: AI tools can be used to optimize the use of natural rubber latex in the mix design of NRLMC. By analyzing data on the properties of natural rubber latex and its interactions with other materials, AI can help to identify optimal materials and formulations to reduce the amount of latex needed while still maintaining the desired properties of NRLMC [27].
iv. Cost optimization: AI can be used to optimize the cost of producing NRLMC. By analyzing data on the prices of raw materials, energy costs, and other factors, AI can help to identify the most cost-effective mix design and production process for NRLMC [28].

In the following sections of this paper, the methodology deployed for this systematic review exercise from essential database expertly selected to relevant literatures is described thus. The next section is critical assessment of mixture design protocols, chemistry and reaction mechanism and rheological properties of the natural rubber latex modified concrete. The subsequent section involves the mechanical properties and morphological assessment of the NRLMC blend and application of neuro-fuzzy models to optimize the NRLMC properties. This section is followed by Gaps in Literatures, conclusion and recommendations for future works in NRLMC.

2. Methodology

In order to achieve the review process in this study, PRISMA which denotes preferred reporting items for systematic reviews and meta-analyses were deployed for this investigative study. PRISMA provides a structured approach to searching for and selecting relevant studies extracting data and synthesizing the findings [29]. The essence is to clearly identify or define the review aims and problems to be addressed, develop detailed protocol and outlining the search strategy in terms of inclusion and exclusion criteria and data extraction methods [30]. Also, the approach of conducting comprehensive search of multiple databases to identify relevant studies in a reproduceable and systematic manner and screening of the identified studies based on predefined inclusion and exclusion criteria from the abstract, titles, keyword and full-text. In this study, databases such as PubMed, Science Direct, Scopus, and Web of Science were deployed and also, keywords with synonyms such as 'natural rubber latex', 'rubber latex modified concrete', rubber latex concrete reaction mechanism', 'microstructural assessment', 'concrete workability', and 'rubber latex concrete

structural properties' combined Boolean logic operators like 'AND' and 'OR'. Using a standardized data extraction procedure, the relevant data were extracted from the included study, the quality assessed using predefined set of biases and synthesize the findings using appropriate statistical methods so as to provide a robust and reliable summary of the available evidence [31]. The overview of the article search strategy and methodology flowchart is presented in *Fig. 2*. Taking into account the aforementioned factors, 6490 pertinent and related published literature authored in English language obtained from scholarly research database and indexing systems were considered with 2354 based on titles and abstract, 2158 based on keyword and 1973 based on full-text. After the screening process, 153 relevant literatures were finally selected for this research which involves 45 review articles and 108 technical papers.

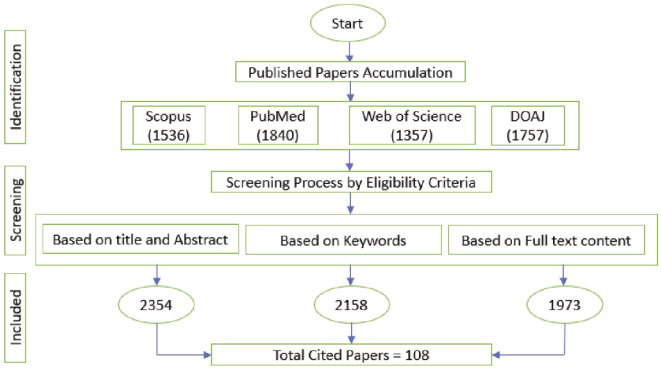

Fig. 2 Relevant Articles selection Strategy and Methodology Flowchart
2. ábra A vonatkozó cikkek kiválasztásának stratégiai és módszertani folyamatábrája

3. Findings of the Surveyed Articles

3.1 Chemistry and Reaction Mechanism of NRL mixture in concrete

The chemistry and reaction mechanism of natural rubber latex (NRL) modified concrete involve several processes that occur at different stages of the mixing and curing process. The addition of NRL to concrete affects the physicochemical behavior of the mixture, resulting to improved mechanical and durability properties [32, 33]. At mixing stage, the NRL particles are dispersed in water and then added to the concrete mix. The NRL particles contain a mixture of proteins, lipids, and carbohydrates that can interact with the cement particles and the water in the mixture. The NRL particles can act as a plasticizer, reducing the water demand of the mixture and improving its workability [34, 35].

During the curing process, interactions occur between NRL particles and Ca^{2+} in cement hydrate, resulting in the formation of a complex that improves the mechanical and durability properties of concrete [34]. Although the exact reaction mechanism is not fully understood, it is believed that NRL reacts with calcium hydroxide produced during cement hydration, forming additional calcium silicate hydrate (C-S-H) gel that contributes to strength enhancement [36, 37]. NRL also acts as a protective barrier around cement particles, reducing water ingress and the entry of aggressive agents into the concrete. The chemical and physical properties of NRL modified concrete are influenced by factors such as NRL type, quantity, mix design, and curing conditions [38]. Further research is needed to fully comprehend the complex chemistry and reaction mechanisms of NRL modified concrete and optimize its performance [39, 40]. The physicochemical characterization of NRLMC involves the study of various properties of the material, including essential factors such as;

- Chemical composition: NRLMC contains a complex mixture of components, including natural rubber latex, cement, aggregates, and water. The chemical composition of the NRL can affect the physical and chemical properties of the concrete [41].
- Rheology: The rheological properties of NRLMC affect its workability and flow behavior. The addition of NRL can modify the rheological properties of the concrete, resulting in a more cohesive and flowable mix [35].
- Hydration kinetics: The addition of NRL to the concrete mix can affect the kinetics of cement hydration. NRL can interact with the cement particles, which can modify the rate of hydration and the formation of hydrates [42]. NRL can interact with other components of the concrete mix, such as the cement and aggregates. These chemical interactions can affect the properties of the NRLMC, including its strength, durability, and resistance to chemical attack [43].

Overall, the physicochemical characterization of NRLMC is essential to understand its properties and behavior in different applications. The characterization of NRLMC can provide insights into the mechanisms that govern its performance, which can be useful for optimizing the mix design and improving the durability and sustainability of the material [44].

Characteristics	Results
Color	White
Total solid content (% by Mass)	50-61.5
Dry Rubber content (% by Mass)	>60
Non-Rubber solid content (% by Mass)	1.35-1.5
KOH (% by Mass)	0.35-0.55
Ammonia content NH_3 (% by Mass)	0.45-0.70
Mechanical stability time (Seconds)	600-1310
Volatile Fatty acid (% by Mass)	0.015-0.1
Magnesium content (% by Mass)	6.5-8
pH	10.05-13.5
Coagulum content (% by Mass)	0.005-0.01
Sludge content (% by Mass)	0.005-0.01
Cu content (PPM)	3.5-6
Fe content (PPM)	5.5-8
Rubber Latex Particle size ()	0.2
Rubber latex specific gravity	0.82-0.98

Table 1 Physicochemical analysis of Natural Rubber Latex Concentrate [36, 37]
1. táblázat Természetes gumi latex koncentrátum fizikai-kémiai elemzése [36, 37]

3.2 Principles of Latex Modification and Mixture design Methodology

When latex is incorporated into mixes with Portland cement, aggregates, and water, the resulting fresh concrete exhibits similar consistency and workability to conventional concrete. After the curing process, the latex-modified concrete (LMC) consists of hydrated cement and aggregate interconnected by a continuous latex film [45, 46]. This film contributes to the superior physical and chemical properties of LMC. According to Ohama [47], the internal responses of latex systems in cement paste and concrete can be divided into three stages. In the first stage, the small polymer latex particles uniformly mix with the fresh cement paste, partially coating the cement grains and early hydration products. In the second stage, as cement hydration progresses and water content reduces, the remaining polymer particles flocculate and form close-packed layers on available surfaces. In the third stage, as water further depletes, the close-packed layers of polymer particles condense to form continuous films or membranes that interpenetrate throughout the cement hydration products [48]. These films transform the fine cement paste matrix into a cement-polymer film matrix. While the details and timeframes of these processes remain speculative, the effect of latex on the transition zone surrounding aggregates in concrete or mortar has not been addressed by Ohama, though it is likely modified [49].

The mix design of NRLMC is an important aspect of its production, as it can considerably influence the behavior and performance of the material [50]. The mix design for NRL modified concrete is typically based on the same principles as conventional concrete, but with modifications to account for the presence of NRL. The mix design for NRL modified concrete typically involves the following steps:

Selection of materials: The materials used in NRLMC are similar to those used in conventional concrete, including cement, aggregates, water, and NRL. The type and properties of these materials can affect the performance of the NRL modified concrete, so careful selection is important [51].

Proportioning of materials: The proportions of the materials used in NRLMC are typically determined based on the desired properties and performance of the material. The amount of NRL added to the mixture can vary depending on the application and the desired performance characteristics [52].

Mixing: The mixing of NRL modified concrete is similar to that of conventional concrete, but care must be taken to ensure that the NRL is evenly dispersed throughout the mixture. NRL can act as a plasticizer, reducing the water demand of the mixture and improving its workability [53].

Curing: The curing of NRL modified concrete is typically done in a similar manner as conventional concrete, but with modifications to account for the presence of NRL. Proper curing is important to ensure the development of the desired mechanical and durability properties [54].

The mix design for NRL modified concrete can vary depending on the specific application and performance requirements. Careful consideration should be given to the selection and proportioning of materials to ensure that the NRL modified concrete meets the desired performance characteristics [55].

3.3 Rheological Characteristics of NRLMC

Rheology investigates the flow and deformation characteristics of materials, including NRLMC. Incorporating NRL into concrete has implications for its rheological properties, such as workability, viscosity, and yield stress [56]. Various techniques, such as slump tests, flow table tests, and rheometer measurements, have been employed to study the rheology of NRLMC [57, 58]. Slump tests assess concrete workability, and NRL addition can enhance it by acting as a lubricant, reducing particle friction and improving flow [59]. However, excessive NRL addition can reduce workability due to increased viscosity and particle friction. Flow table tests measure workability too, and NRL incorporation can increase the spread diameter, indicating improved flow. Yet, excessive NRL can reduce the spread diameter and hinder flowability [60, 61]. Rheometer measurements offer detailed rheological insights. NRL addition can elevate viscosity, signifying enhanced resistance to deformation. It can also elevate the yield stress, improving stability and mitigating segregation and bleeding risks [62]. While NRL inclusion influences the rheological properties of concrete, the optimal NRL dosage depends on specific mix designs and application requirements, as excessive NRL can negatively impact rheology [63].

3.3.1 Workability Property

NRLMC offers numerous advantages over traditional concrete and holds promise for various applications, including building and infrastructure construction. NRL, obtained from renewable sources, renders NRLMC an environmentally friendly choice [64]. The incorporation of NRL enhances the workability of concrete, a crucial attribute in the construction sector. Good workability facilitates easier handling, placement, and finishing of the concrete mix, reducing the required effort [65, 66]. NRL enhances concrete workability by reducing water demand and increasing mix cohesion, leading to easier placement and improved surface finish [67]. It also improves flowability and pumpability, particularly useful for transporting concrete over long distances or through narrow spaces [68]. NRLMC's workability is a key property improved by adding NRL, reducing water demand and achieving a more cohesive mix [69]. Multiple studies confirm the superior workability of NRLMC compared to traditional concrete. For instance, adding 10% NRL increased workability by around 21% while reducing the water-cement ratio by approximately 18% [70]. NRL effectively enhances concrete workability, offering advantages in placement, finishing, and transportation. The improved workability of NRLMC can result in several benefits for construction projects [70]. A more workable mix can be easier to place and finish, which can reduce the amount of labor required for concrete placement. It can also result in a more uniform and consistent concrete surface, with fewer defects or imperfections [70]. However, it is important to note that the workability of NRLMC can be affected by several factors, including the type and dosage of NRL used, the mix design, and the environmental conditions. Therefore, it is essential to carefully design and test the mix to achieve the desired workability properties [71].

3.4 Mechanical Behavior of NRLMC

The addition is NRL to concrete can improve its mechanical properties, such as compressive strength, flexural strength, and durability by increased toughness behavior of the concrete whereby NRL act as crack inhibitors by absorbing energy during deformation [72]. Also, NRL can act as adhesive agent to improving the bond strength between the cement paste and the aggregates, and increase the ductility property of the concrete making it more resistant to brittle fracture [73]. Moreover, addition of NRL enhances the abrasion resistance capacity of the concrete and lower the permeability property by reducing ingress of water and other harmful substances which can lead to deterioration and premature failure of the structure [74].

3.4.1 Compressive Strength Properties of NRLMC

The compressive strength of concrete is a critical mechanical property that reflects its ability to withstand compressive loads. Research indicates that incorporating NRL can enhance the compressive strength, particularly in early stages, owing to improved concrete microstructure and enhanced cement hydration [75]. However, excessive NRL addition can reduce compressive strength due to the high viscosity of NRL hindering particle movement and mix compaction. Notably, Subash et al. demonstrated that the addition of 5% NRL resulted in a 20% increase in compressive strength at 40MPa. These findings highlight the positive impact of NRL on concrete's compressive strength, attributing it to improved microstructure and cement hydration. Particles can fill the voids between cement particles, resulting in a denser and more compact concrete matrix [72]. The improvement in compressive strength is mainly attributed to the following mechanisms:

i. Pozzolanic reaction: NRL can react with the calcium hydroxide produced during cement hydration, forming additional (C-S-H) gel that can contribute to the strength and durability of the concrete.
ii. Latex film formation: NRL can form a film around the cement particles, which can improve the adhesion and cohesion between the particles, resulting in a stronger and more stable matrix.

Excessive NRL addition can decrease compressive strength due to NRL's high viscosity impeding particle movement and mix compaction. The optimal NRL dosage relies on factors like NRL type, quantity, mix design, and curing conditions. Typically, adding NRL at 5-10% by weight of cement achieves substantial enhancement in compressive strength while preserving workability and other concrete properties [76].

3.4.2 Flexural Strength Properties of NRLMC

The flexural strength of concrete is crucial as it demonstrates its resistance to bending and tension loads. Research indicates that adding NRL can enhance the flexural strength, particularly in early stages, owing to improved microstructure and the formation of NRL-cement complexes that provide a stable and cohesive matrix [77]. However, excessive NRL addition, similar to compressive strength, can diminish flexural strength. NRL's presence fills voids between cement particles, resulting in a more compact and homogeneous matrix, enhancing adhesion and cohesion and consequently leading to a stronger and more stable structure [78]. The improvement in flexural strength is mainly attributed to the following mechanisms:

i. Increased tensile strength: NRL can improve the tensile strength of the concrete, which is a key factor in determining its flexural strength.
ii. Increased interparticle bonding: NRL can form a film around the cement particles, improving the interparticle bonding and resulting in a stronger and more stable matrix.
iii. Enhanced microstructure: The addition of NRL can result in a more homogeneous and compact microstructure, which can improve the load transfer and reduce the risk of cracking and failure.

The optimal fraction of NRL to be incorporated in the matrix to improve the flexural strength of concrete varies depending on various factors, such as the nature and quantity of NRL, the mix design, and the curing conditions [79]. Similar to compressive strength behavior, the inclusion of NRL at a measure limit of 5-10% by cement mass can result in a substantial enhancement in flexural strength properties to about 5.27 N/mm2 while preserving other concrete's characteristics which is in consonance with the findings of Grinys et al [56].

3.4.3 Durability Properties of NRLMC

Durability is a significant mechanical property of concrete, representing its ability to withstand environmental factors like freeze-thaw cycles, chloride ion penetration, and carbonation. Research has demonstrated that incorporating NRL can enhance concrete durability by improving microstructure and forming NRL-cement complexes that create a protective layer on the concrete surface [80]. Adding NRL to concrete improves its ability to resist deterioration caused by moisture, freeze-thaw cycles, chemical attack, and abrasion. Additionally, NRL incorporation influences other mechanical properties such as elastic modulus, Poisson's ratio, fatigue resistance, and fracture toughness, resulting in a more resilient material less prone to cracking or spalling [76]. Notably, studies have confirmed that NRL addition enhances concrete durability, particularly in harsh environments, as NRL acts as a protective barrier against aggressive agents like water and chemicals that can penetrate and deteriorate the concrete [71].

3.4.4 Strength Development Properties

The incorporation of NRL into concrete can influence its strength development characteristics. Generally, NRL addition enhances early-age strength, while the impact on long-term strength varies depending on factors like mix design, NRL dosage, and curing conditions [81]. Research indicates that NRL incorporation can increase the compressive strength of concrete, particularly in the early curing stages. This improvement stems from enhanced bonding between cement and NRL particles, as well as improved workability, leading to better compaction and reduced voids in the concrete [82]. The effect of NRL on flexural strength is less conclusive and

subject to specific application and performance requirements. Some studies show an increase in flexural strength with NRL addition, while others report no significant effect or even a decrease. It is crucial to consider multiple factors, including curing conditions, water-cement ratio, cement type, and mix design, as they can influence the strength development properties of NRL-modified concrete. Therefore, careful control of these factors and appropriate testing are necessary to determine the optimal mix design and curing conditions for a given application [83].

3.5 Microstructural Behaviors Assessments

The microstructural assessment of NRLMC involves the study of the concrete at the microscopic level, focusing on the interaction between the different components' mix and their effect on the microstructure of the hardened concrete [84]. Some of the key aspects of the microstructure of NRLMC are:

i. Cement matrix: The cement matrix is the primary component of the NRLMC microstructure, and it is responsible for providing the strength and durability of the concrete. The addition of NRL to the mix can modify the microstructure of the cement matrix, resulting in a more compact and homogeneous structure [85].
ii. Aggregates: The aggregates in NRLMC can affect the microstructure of the concrete by providing mechanical interlocking and improving the strength of the concrete. The addition of NRL can also improve the bonding between the aggregates and the cement matrix, resulting in a stronger and more durable concrete [65].
iii. NRL: The addition of NRL to the mix can modify the microstructure of the concrete by forming a thin film around the cement particles. This film can improve the bonding between the cement and aggregates and result in a more cohesive and compact microstructure [58].
iv. Porosity: The porosity of the NRLMC microstructure can affect the durability and strength of the concrete. The addition of NRL can reduce the porosity of the concrete by improving the packing of the cement matrix and reducing the amount of water needed for the mix [71].

Overall, the microstructural assessment of NRLMC is important to understand the interaction between the different components of the mix and how they affect the properties of the concrete. This knowledge can be used to optimize the mix design and improve the durability and sustainability of the concrete. Techniques such as SEM and XRD can be used to study the microstructure of NRLMC in detail [33].

3.5.1 Scanning electron microscopy (SEM)

Scanning electron microscopy (SEM) is a highly effective technique for examining the microstructure of NRLMC. It enables high-resolution imaging of the concrete's surface and cross-section, offering detailed insights into the morphology and structure of its various components [86]. In SEM analysis of NRLMC, a small section of the concrete sample is typically prepared, coated with a conductive material like gold or carbon, and placed in the SEM chamber. A beam of electrons is then scanned over the sample's surface, generating secondary electrons that are detected by a sensor to produce an image of the concrete's surface [87]. SEM analysis is a valuable tool for understanding the microstructure of NRLMC and its impact on properties. This information can be used to optimize mix design and enhance concrete's strength, durability, and sustainability [88]. In *Fig. 3*, the concrete sample without NRL displayed irregular-shaped aggregates, micro cracks, and pores. In contrast, the NRL-modified concrete exhibited needle-like ettringite and calcium hydroxide crystals near the aggregate interface. NRL particles were observed as lumps deposited on hydrated products, forming a dense microstructure that filled capillary pores and created a membranous film [89].

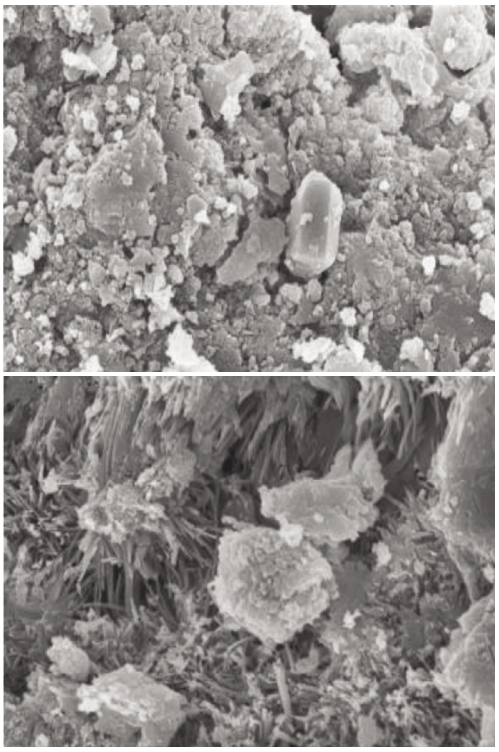

Fig. 3 SEM image of a) Control Specimen (CS) b) 5% Latex [87]
3. ábra A (CS) kontrollminta (a) és az 5% Latex tartalmú minta SEM felvétele [87]

3.5.2 X-ray diffraction (XRD)

XRD is a valuable technique for analyzing the microstructure of NRLMC. It provides information about the crystallographic structure and phase composition of the materials in the mix. XRD can identify the phases present, such as calcium silicate hydrates (C-S-H) and calcium hydroxide ($Ca(OH)_2$), and quantify their relative amounts and crystallographic properties [90]. The addition of NRL can result in new peaks or modifications to existing peaks in the XRD pattern, indicating changes in the mix's crystallographic structure [91]. XRD analysis can be used to optimize the mix design and enhance the concrete's strength, durability, and sustainability. XRD can track the formation and evolution of hydrated products, revealing that NRL modifies the crystallographic structure of the C-S-H phase, resulting in a more compact and ordered microstructure [92]. The XRD spectra of hydrated NRLMC specimens display peaks representing $Ca(OH)_2$, $CaCO_3$,

calcium silicate (Ca_2SiO_4), and quartz. The presence of quartz as the main crystalline phase and traces of un-hydrated Ca_2SiO_4 are observed. These findings highlight the impact of NRL on the crystalline phases during the hydration curing process [93].

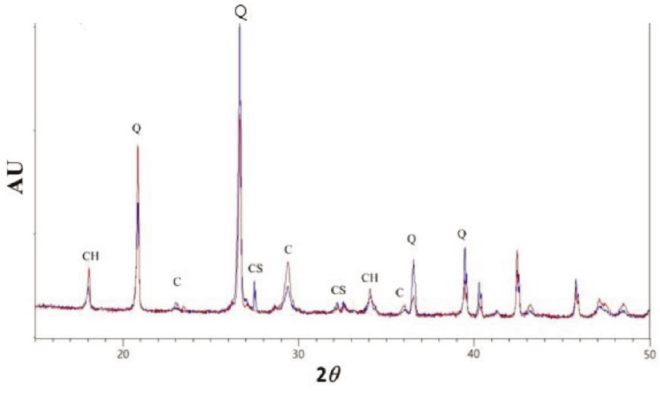

Fig. 4 X-ray diffraction pattern of NRL modified concrete specimen [54]
4. ábra Az NRL módosított betonminta röntgendiffraktogramja [54]

4. Optimization and Modeling of the Mechanical Properties of NRMLC

4.1 Adaptive Neuro Fuzzy Inference System (ANFIS)

The Adaptive Neuro Fuzzy Inference System (ANFIS) is an AI approach that combines neural networks and fuzzy logic to create a hybrid system capable of learning and decision-making. Introduced by Jang in 1993, ANFIS has found applications in control, classification, and prediction [93]. It comprises two key components: a fuzzy inference system and a neural network. The fuzzy inference system utilizes fuzzy rules and membership functions to map inputs to outputs, while the neural network fine-tunes the fuzzy system's parameters for optimal performance [94]. ANFIS is a supervised learning method that trains on input/output data. By adjusting parameters, it minimizes prediction errors. Trained ANFIS models can then forecast outputs for new data [95]. ANFIS boasts benefits such as handling complex relationships and adapting to changing input data. Its versatility extends to fields like engineering, finance, and medicine [96, 97]. ANFIS finds extensive application in engineering for modeling and control, including in the case of NRLMC. For NRLMC mix design optimization, ANFIS develops a model that correlates input parameters (e.g., NRL amount, cement, water, aggregate) to output properties (e.g., compressive strength, flexural strength, durability). This model helps determine optimal mix designs for desired NRLMC properties [98]. Additionally, ANFIS can predict mechanical properties of NRLMC based on input mix design parameters, avoiding costly and time-consuming lab tests. This significantly reduces NRLMC research and development costs and time. Employing ANFIS in NRLMC enables efficient mix design optimization and accurate mechanical property prediction, leading to superior performance in construction applications [99, 100].

4.1.1 ANFIS Network Architecture

The ANFIS architecture employs a training process to adjust the parameters of the fuzzy sets and neural network, learning the relationships between input and output variables. This is achieved through backpropagation, a gradient descent algorithm that minimizes prediction errors [101]. ANFIS combines artificial neural networks and fuzzy logic, consisting of five layers: input, fuzzification, normalization, defuzzification, and output [102, 103]. The input layer receives system input variables and passes them to the next layer. The fuzzification layer converts crisp inputs to fuzzy values using membership functions. Each node in this layer represents a fuzzy set and applies a membership function [104]. The normalization layer evaluates fuzzy rules derived from expert knowledge or data, ensuring equal importance among nodes in the subsequent layer [105, 106]. The defuzzification layer converts fuzzy sets back to crisp values, representing the system output. Each node represents a rule, computing its strength based on inputs and membership functions. The output layer combines rule strengths and computes the final output [107, 108].

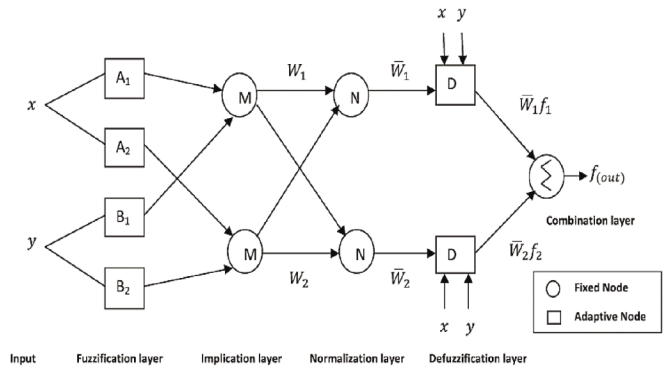

Fig. 5 ANFIS basic architecture [105]
5. ábra ANFIS alap architektúra [105]

5. Identified Gaps in Reviewed Literatures

While there has been significant researches on natural rubber latex modified concrete, there are still some gaps in the literature that require further investigation. Some of the major gaps include:

i. Long-term durability: Although some studies have investigated the durability of natural rubber latex modified concrete, more research is needed to assess its long-term performance under different environmental conditions.

ii. Optimization of mix design: There is a need for more research to optimize the mix design of natural rubber latex modified concrete, particularly with respect to the proportion of natural rubber latex, cement, and aggregate to achieve the desired properties.

iii. Mechanical properties: While some studies have investigated the compressive and flexural strength of natural rubber latex modified concrete, more research is needed to assess its other mechanical properties, such as tensile strength, modulus of elasticity, and impact resistance.

iv. Rheological properties: More research is needed to investigate the rheological properties of natural rubber latex modified concrete, including its workability, flowability, and setting time.

v. Cost-benefit analysis: While the use of natural rubber latex modified concrete has many potential benefits, such as improved durability and reduced environmental impact, there is a need for more research to assess its overall cost-effectiveness compared to traditional concrete.

Addressing these gaps in the literature will help to further advance the development and application of natural rubber latex modified concrete in various construction projects. Furthermore, considering the application of soft computing techniques deployed in the optimization of structural properties of NRLMC, while there have been some studies on the application of artificial intelligence, specifically the ANFIS, in the optimization of NRLMC, there are still some gaps in the literature, such as:

i. Lack of studies comparing the performance of ANFIS with other machine learning techniques in the optimization of NRLMC.
ii. Limited studies on the use of ANFIS in the optimization of other properties of NRLMC, such as durability and workability.
iii. Limited studies on the use of ANFIS in the optimization of NRLMC using different types and grades of natural rubber latex.
iv. Lack of studies on the optimization of NRLMC using ANFIS with the consideration of sustainability factors, such as the use of recycled materials or reducing the carbon footprint.
v. Lack of studies on the application of ANFIS in the optimization of NRLMC in different environmental conditions, such as high temperatures or exposure to chemicals.

Addressing these gaps could provide a better understanding of the capabilities and limitations of ANFIS in the optimization of NRLMC, and could contribute to the development of more efficient and sustainable construction materials.

6. Conclusion

To summarize, natural rubber latex modified concrete offers improved mechanical, durability, and workability properties due to enhanced bonding and microstructure. Optimizing mix design, curing conditions, and compaction factor is crucial. ANFIS have shown promise in optimizing mix design and predicting mechanical properties. However, further research is needed to understand the long-term durability and behavior of the material under different environmental conditions. Exploring the use of additional additives alongside natural rubber latex could further enhance the material's properties.

7. Acknowledgements

The authors of this review article acknowledge the supports of Federal University of Technology Owerri, Imo state Nigeria and University of Cross River State, Nigeria for the PhD studies of Efiok Etim Nyah.

References

[1] Imtiaz, L.; Rehman, S.K.U.; Memon, A.S.; Khizar, K.M.; Faisal, J.M. A Review of Recent Developments and Advances in Eco-Friendly Geopolymer Concrete. Appl. Sci. 2020, 10, 7838.
[2] Ganesan, N. and Sreekala.R., Fracture characteristics of latex modified SFRC, Journal of Structural Engineering, April 1999, Vol. 26, No. 1, pp. 49-54.
[3] Neelamegam, M. Dattatreya, J.K. Rajmane, N.P. Peter, J.A. and Gopalakrishnan, S., Development of durable concrete using natural rubber latex, Indian Concrete Journal, August 2000.
[4] Bala M., Ismail M. (2012). "Influence of non-hydrocarbon substances on the compressive of Natural rubber latex modified concrete", ELSEVIER Journal of Construction and Building Materials, Vol 27, pp 241-246
[5] Nagraj T, S., Iyengar R., Rao K. (2010). "Super plasticized natural rubber latex modified concrete", Cement and Concrete Research, Vol 18 (1), pp 138-144
[6] Khamput P., Suweero K. (2011). "Properties of Mortar mixing with Medium Ammonia concentrated latex", Energy Procedia, Vol 9, pp 559-567
[7] Bala M., Ismail M. (2012). "Performance of Natural rubber latex modified concrete in acidic and sulphated environments", ELSEVIER Journal of Construction and Building Materials, Vol 31, pp. 129-134
[8] M. S. Shobha (2014). "Mechanical Properties of latex modified high performance concrete." IOSR Journal of Mechanical and Civil Engineering, Vol. 11, pp. 13-19
[9] Ravindra Rajha, R., Effect of the natural rubber latex on the Portland cement paste-mortar and concrete, Proceeding of the Third International Congress on Polymers in Concrete, Tokyo, Japan, May1981, Vol. 1, pp. 380 – 394.
[10] Hadi MN, Zhang H, Parkinson S (2019) Optimum mix design of geopolymer pastes and concretes cured in ambient condition based on compressive strength, setting time and workability. J Build Eng 23:301–313
[11] Pu-woei Chen, Xuli Fu, and Chung, D.D.L., Micro structural and mechanical effects of latex-methyl cellulose and silica fume on carbon fibre reinforced cement, ACI Materials journal, Mar-April1 997, Vol. 94, No. 2, pp. 147-155.
[12] Bala M., Ismail M., Haron Z. (2011). "Elastomeric effect of natural rubber latex on compressive strength of concrete at high temperatures", ASCE Journal of Materials in Civil Engineering, Vol 23, pp 1697-1702
[13] SivaKumar, M.V.N. (2011), "Effect of Polymer modification on mechanical and structural properties of concrete "– An experimental investigation, IJCSE, 1(04), 732-740.
[14] Han, J. W., Lee, S. K., Jeon, J. H., Yu, C., Oh, R. O. and Park, C. G., (2015). "Strength and durability of latex modified jute/macro-synthetic hybrid fibre-reinforced concrete." Materials Research Innovations, 19(5), S5- 894-S5-897.
[15] S. S. Sharma and S. Kumar, "Study on mechanical and durability properties of crumb rubber modified concrete," Journal of Materials in Civil Engineering, vol. 30, no. 1, pp. 04017258, Jan. 2018.
[16] A. H. A. Al-Deen, H. M. Al-Kindi, and H. A. Al-Saidy, "Rubberized concrete: A review on its properties, applications and challenges," Construction and Building Materials, vol. 224, pp. 920-939, Apr. 2019.
[17] Rolere, C., Le Maou, F., & Khelidj, A. (2016). Mechanical and thermal properties of cement mortar with addition of natural rubber latex. Construction and Building Materials, 110, 87-96. https://doi.org/10.1016/j.conbuildmat.2016.02.020.
[18] Khamput, P., Jaturapitakkul, C., & Kiattikomol, K. (2011). Use of natural rubber latex in concrete containing rice husk ash as a pozzolanic material. Construction and Building Materials, 25(1), 1-6. https://doi.org/10.1016/j.conbuildmat.2010.05.037.
[19] Rao, G. V., Sudhakara Reddy, B., Sireesh, S., Ramesh Babu, P., & Venkateswara Rao, P. (2013). Studies on mechanical properties of concrete with rice husk ash and natural rubber latex. Construction and Building Materials, 41, 312-319. https://doi.org/10.1016/j.conbuildmat.2012.11.008.
[20] K. C. Onyelowe, E. J. Fazal, E. O. Michael, C. O. Ifeanyichukwu, G. U. Alaneme, and I. Chidozie, "Artificial intelligence prediction model for swelling potential of soil and quicklime activated rice husk ash blend

for sustainable construction," Jurnal Kejuruteraan. 33(4) 2021: 845-852 https://doi.org/10.17576/jkukm-2021-33(4)-07.

[21] Ujong, J.A., Mbadike, E.M. & Alaneme, G.U. Prediction of cost and duration of building construction using artificial neural network. Asian J Civ Eng (2022). https://doi.org/10.1007/s42107-022-00474-4

[22] Armaghani, D. J., & Asteris, P. 2020. A comparative study of ANN and ANFIS models for the prediction of cement-based mortar materials compressive strength. Computer Science: Neural Computing and Applications, Corpus ID: 221110523. 10.1007/ s00521-020-05244-4

[23] Ganasen, N., Krishnaraj, L., Onyelowe, K.C., Alaneme, G. U. et al. Soft computing techniques for predicting the properties of raw rice husk concrete bricks using regression-based machine learning approaches. Sci Rep 13, 14503 (2023). https://doi.org/10.1038/s41598-023-41848-1

[24] R.Karthikeyan, Ma Atmanandi, K. Suguna and P.N. Raghunath. ANFIS Based Modeling for Performance Evaluation of Rubberized Concrete Beams. Journal of Electronics Information Technology Science and Management. volume 12, issue 11, 2022. Pp. 234-247.

[25] Alaneme George, U. & Mbadike Elvis, 'Modelling of the mechanical properties of concrete with cement ratio partially replaced by aluminium waste and sawdust ash using artificial neural network', M. SN Appl. Sci. (2019) 1: 1514. https://doi.org/10.1007/s42452-019-1504-2

[26] Reddy, K. N., Kumar, A., & Reddy, B. S. (2017). Prediction of splitting tensile strength of rubber latex concrete using ANFIS. Journal of Materials in Civil Engineering, 29(4), 04016243. https://doi.org/10.1061/(ASCE)MT.1943-5533.0001788.

[27] Hongwei Song, Ayaz Ahmad, Furqan Farooq, Krzysztof Adam Ostrowski, Mariusz Maślak, Slawomir Czarnecki, Fahid Aslam, Predicting the compressive strength of concrete with fly ash admixture using machine learning algorithms, Construction and Building Materials, Volume 308, 2021, 125021, https://doi.org/10.1016/j.conbuildmat.2021.125021.

[28] Obianyo, J.I., Okey, O.E. & Alaneme, G.U. Assessment of cost overrun factors in construction projects in Nigeria using fuzzy logic. Innov. Infrastruct. Solut. 7, 304 (2022). https://doi.org/10.1007/s41062-022-00908-7

[29] O'Dea RE, Lagisz M, Jennions MD, Koricheva J, Noble DWA, Parker TH, Gurevitch J, Page MJ, Stewart G, Moher D, Nakagawa S. Preferred reporting items for systematic reviews and meta-analyses in ecology and evolutionary biology: a PRISMA extension. Biol Rev Camb Philos Soc. 2021 Oct;96(5):1695-1722. https://doi.org/10.1111/brv.12721.

[30] Alawi, Asiya, Abdalrhman Milad, Diego Barbieri, Moad Alosta, George Uwadiegwu Alaneme, and Qadir Bux alias Imran Latif. 2023. "Eco-Friendly Geopolymer Composites Prepared from Agro-Industrial Wastes: A State-of-the-Art Review" CivilEng 4, no. 2: 433-453. https://doi.org/10.3390/civileng4020025

[31] Moher, D., Liberati, A., Tetzlaff, J., & Altman, D. G. (2009). Preferred reporting items for systematic reviews and meta-analyses: The PRISMA statement. PLoS Medicine, 6(7), e1000097. https://doi.org/10.1371/journal.pmed.1000097.

[32] Ahmed M. Diab, Hafez E. Elyamany, Ali Hassan Ali, Experimental investigation of the effect of latex solid/water ratio on latex modified co-matrix mechanical properties, Alexandria Engineering Journal, Volume 52, Issue 1, 2013, Pages 83-98, https://doi.org/10.1016/j.aej.2012.11.002

[33] Vaishali. G. Ghorpade, Sri. K. Munirathnam and H. Sudarsana Rao, "Effect of natural rubber latex on strength and workability of fibre reinforced high-performance - concrete with metakaolin admixture", International Journal of Engineering Research and Applications, Vol. 3, Issue 3,2013, pp.827-831.

[34] Shuyi Yao and Yong Ge, "Effect of Styrene Butadiene Rubber Latex on Mortar and Concrete Properties", Advanced Engineering Forum, Vol. 5, 2012, pp.283-288

[35] Barluenga, G., and Hemandez, F. 2004. SBR latex modified mortar rheology and mechanical behavior. Cement and Concrete Research, 34(3): 527–535. doi:10.1016/j.cemconres.2003.09.006.

[36] H.Sudarsana Rao, K.Munirathnam, Vaishali. G.Ghorpade, and C.Sashidhar "Influence Of Natural Rubber Latex On Permeability Of Fibre Reinforced High-Performance Concrete", International Journal of Innovative Research in Science, Engineering and Technology , Vol. 2, Issue 7, July 2013

[37] Sakdapipanich, J.T. 2007. Structural characterization of natural rubber based on recent evidence from selective enzymatic treatments. Journal of Bioscience and Bioengineering, 103(4): 287–292. https://doi.org/10.1263/jbb.103.287.

[38] Rattanaveeranon S, Dumrongsil S and Jiamwattanapong K (2019). Effect of Latex Rubber and Rubber Powder as an Admixture on Bending Strength of Cement Mortars Appl. Mech. Mater. 891 180–6

[39] Shaji P, Aswathi KP, Hanna P, George JK, Shameer K (2017) Effect of Natural Rubber Latex as admixtures in concrete. Int Res J Eng Technol (IRJET) 4(4):2031–2034

[40] Xu, F., Zhou, M., Chen, J. and Ruan, S., (2014). "Mechanical performance evaluation of polyester fiber and SBR latex compound-modified cement concrete road overlay material." Construction and Building Materials, 63, 142-149.

[41] Harahap H, Hadinatan K, Hartanto A, Surya I and Ginting M 2015 The effect of drying temperature on mechanical properties of natural rubber latex products with cassava peel waste powder modified alkanolamide J. Eng. Sci. Technol 53-63

[42] Keke Sun, Shuping Wang, Lu Zeng, Xiaoqin Peng, Effect of styrene-butadiene rubber latex on the rheological behavior and pore structure of cement paste, Composites Part B: Engineering, Volume 163, 2019, Pages 282-289, https://doi.org/10.1016/j.compositesb.2018.11.017.

[43] T. S. Nagraj, S. R. Iyengar, B. K. Rao (1988). "Super plasticized natural rubber latex modified concrete."Cement and Concrete Research, Vol. 18, pp. 138-144

[44] H. SudarsanaRao, Sasidhar .C, Vaishali.G, Ghorpade. (2013). "Influence of natural rubber latex on permeability of fibre reinforced high performance concrete", International Journal of Innovative Research in Science, Engineering & Technology Vol.2, Issue.7, pp. 2715-2720.

[45] Ramakrishnan V. Synthetic of highway practice 179 – latex modified concrete and mortars. Washington (DC): NCHRP; 1992.

[46] Mohammad I, Bala M, Hamidi MZ. Effects of latex concentrate on strength and drying shrinkage of concrete. In: Proceedings of the Asian pacific structural engineering conferences (APSEC). Langkawi, Malaysia; 2009. p. 665–9. Top of Form

[47] Y. Ohama, "Process technology of latex-modified systems," in Handbook of Polymer-Modified Concrete and Mortars, Elsevier, pp. 22–44, 1995.

[48] Ohama, Y. 1987. Principle of latex modification and some typical properties of latex-modified mortars and concretes. ACI Materials Journal, 86: 511–518.

[49] Boondamnoe O, Oshima M, Azura A R, Chuajuljit S and Ariffin A 2012 Recycling waste natural rubber latex by blending with polystyrene – characterization of mechanical properties Int. J. Mod. Phys.: Conf. Ser. 6 391-396

[50] BS 1881:1986. Testing concrete – part 125. Methods for mixing and sampling fresh concrete in the laboratory. London: BSI Publications.

[51] Japan Industrial Standards JIS1171:2000. Test materials for polymer-modified mortar. Tokyo: Japanese Standard Association.

[52] Xiao, J., Jiang, D., Sha, A. and Huang, Y., (2017). "Effect of styrene – butadiene rubber latex on the properties of modified porous cement – stabilised aggregate." Road Materials and Pavement Design.

[53] Nabavi, F., Nejadi, S. and Samali, B., (2013). "Experimental investigation on mix design and mechanical properties of polymer (latex) modified concrete." Advanced Materials Research, 687, 112- 117.

[54] Zonglin Xie, Qiang Yuan, Hao Yao, Fuwen Zhong, Mengjie Jiang, Hardened properties and microstructure change of sulphoaluminate cement modified with different doses of styrene-butadiene rubber latex, Construction and Building Materials, Volume 400, 2023, 132618, https://doi.org/10.1016/j.conbuildmat.2023.132618.

[55] Ogbonna C., Mbadike E. M. and Alaneme G. U. (2020), Effects of Cassava-Peel-Ash on Mechanical Properties of Concrete. Umudike Journal of Engineering and Technology (UJET); Vol. 6, No. 2, December 2020, pp. 61 – 75. https://doi.org/10.33922/j.ujet_v6i2_8

[56] Grinys, A., Augonis, A., Daukšys, M., & Pupeikis, D. (2020). Mechanical properties and durability of rubberized and SBR latex modified rubberized concrete. Construction and Building Materials. https://doi.org/10.1016/j.conbuildmat.2020.118584

[57] Soliman, E. M., Kandil, U. F., & Reda Taha, M. M. (2011). A new latex modified mortar incorporating carbon nanotubes: Preliminary investigations (Vol. 278). Michigan: ACI Special Publications.

[58] Wang R, Lackner R and Wang P M 2011 Effect of styrene-butadiene rubber latex on mechanical properties of cementitious materials highlighted by means of nanoindentation Strain 47 117–26

[59] Vo M L and Plank J 2018 Evaluation of natural rubber latex as film forming additive in cementitious mortar Constr. Build. Mater. 169 93–9

[60] Chimmaobi, O., Mbadike, E. M. and Alaneme, G. U. (2020). Experimental Investigation of Cassava Peel Ash in the Production of Concrete and Mortar, Umudike Journal of Engineering and Technology; Vol. 6, No. 2, December 2020, pp. 10 – 21; https://doi.org/10.33922/j.ujet_v6i1_1

[61] M. Nibin Gafoor and P. R. Beena, Effect of Natural Rubber Latex in concrete with Metakaolin Admixture: In Book - Recent Advances in Materials, Mechanics and Management, Hamburg, Germany, 1 edition, 2019.

[62] Shiyun Zhong, Zhiyuan Chen, Properties of latex blends and its modified cement mortars, Cement and Concrete Research, Volume 32, Issue 10, 2002, Pages 1515-1524, https://doi.org/10.1016/S0008-8846(02)00813-X.

[63] Z. S. Al-Khafaji, M. W. Falah, A. A. Shubbar et al., "The impact of using different ratios of latex rubber on the characteristics of mortars made with GGBS and Portland cement," IOP Conference Series: Materials Science and Engineering, vol. 1090, no. 1, Article ID 12043, 2021.

[64] Vinaya K L, Sanjith J, Ranjith A and Kiran B M, "Effect of natural rubber latex on Normal strength concrete", International Journal of Advance Research In Science And Engineering, Vol. No.3, Issue No.9, 2014, pp.334-355

[65] S. Zhong and Z. Chen, "Properties of latex blends and its modified cement mortars," Cement and Concrete Research, vol. 32, no. 10, pp. 1515–1524, 2002.

[66] U. Alaneme George and M. Mbadike Elvis, (2019) optimization of flexural strength of palm nut fibre concrete using Scheffe's theory, Materials Science for Energy Technologies 2 (2019) 272–287. https://doi.org/10.1016/j.mset.2019.01.006.

[67] K. Sanjayan, N. N. Kumaran, and L. V. Krishnan, "Rubber-modified concrete: A state-of-the-art review," Journal of Materials in Civil Engineering, vol. 23, no. 4, pp. 451–460, Apr. 2011.

[68] Feng Liu, Guixuan Chen, Lijuan Li, "Impact performance of rubber", Journal reinforced of construction and building materials 36 (2012) 604 - 616.

[69] Ankur C. Bhogayata, Narendra K. Arora, Workability, strength, and durability of concrete containing recycled plastic fibers and styrene-butadiene rubber latex, Construction and Building Materials, Volume 180, 2018, Pages 382-395, https://doi.org/10.1016/j.conbuildmat.2018.05.175.

[70] Uzoma Ibe Iro, George Uwadiegwu Alaneme, Abdalrhman Milad, Bamidele Charles Olaiya, Obeten Nicholas Otu, Edward Uchenna Isu, and Magnus Nnaemeka Amuzie. (2022). Optimization and Simulation of Saw Dust Ash Concrete Using Extreme Vertex Design Method. Advances in Materials Science and Engineering Volume 2022, Article ID 5082139, 22 pages https://doi.org/10.1155/2022/5082139

[71] M. S. Shobha, C. Shashidhar, H. S. Rao (2013). Strength studies of Natural Rubber latex modified High performance concrete. International Journal of Engineering Research & Technology, Vol. 2, pp. 1836-1852

[72] Gampanart Sukmak, Patimapon Sukmak, Suksun Horpibulsuk, Teerasak Yaowarat, Kittipong Kunchariyakun, Orasa Patarapaiboolchai, Arul Arulrajah, Physical and mechanical properties of natural rubber modified cement paste, Construction and Building Materials, Volume 244, 2020, 118319, https://doi.org/10.1016/j.conbuildmat.2020.118319.

[73] Zhan, Y., Lavorgna, M., Buonocore, G. G. & Xia, H. Enhancing electrical conductivity of rubber composites by constructing interconnected network of self-assembled graphene with latex mixing. J. Mater. Chem. 22, 10464–10468 (2012).

[74] S. K. M. Pothinathan, M. Muthukannan, S. Narayanan, "Comparison of bond strength analysis on the interfacial layer of old and new concrete using latex, epoxy and glycoluril," IOP Conf. Ser. Mater. Sci. Eng., vol. 983, p. 012006, 2020. https://doi.org/10.1088/ 1757-899X/983/1/012006

[75] Han, J.-W.; Jeon, J.-H.; Park, C.-G. Mechanical and Permeability Characteristics of Latex-Modified Pre-Packed Pavement Repair Concrete as a Function of the Rapid-Set Binder Content. Materials 2015, 8, 6728–6737.

[76] S. Subash, K. M. Mini, and M. Ananthkumar, "Incorporation of natural rubber latex as concrete admixtures for improved mechanical properties," Materials Today: Proceedings, vol. 46, pp. 4859–4862, 2021.

[77] Won J.P., Kim J.H., Lee S.W., Park C.G. Durability of Low-Heat, Ultra Rapid-Hardening, Latex Modified Polymer Concrete. Prog. Rubber Plast. Recycl. Technol. 2009;25:91–102. https://doi.org/10.1177/147776060902500201.

[78] Kim, D-H. and Park, C-G., (2013). "Permeability, abrasion, and impact resistance of latex-modified fiber reinforced concrete for precast concrete pavement applications." Progress in Rubber, Plastics and Recycling Technology, 29(4), 239-254.

[79] P. O. Awoyera, F. Althoey, H. Ajinomisan et al., "Potential of natural rubber latex in cement mortar for thermal insulating material in buildings," Front. Mater.vol. 10, Article ID 1152492, 2023.

[80] Diab, A. M., Elyamany, H. E. and Ali, A. H., (2013). "Experimental investigation of the effect of latex solid/water ratio on latex modified co-matrix mechanical properties." Alexandra Engineering Journal, 52, 83-98.

[81] Alaneme, G.U., Olonade, K.A. & Esenogho, E. Eco-friendly agro-waste based geopolymer-concrete: a systematic review. Discov Mater 3, 14 (2023). https://doi.org/10.1007/s43939-023-00052-8

[82] Kim D.H., Park C.G. Strength, permeability and durability of hybrid fiber-reinforced concrete containing styrene butadiene latex. J. Appl. Polym. Sci. 2013;129:1499–1505. https://doi.org/10.1002/app.38861.

[83] George Uwadiegwu Alaneme & Elvis Michael Mbadike (2021) optimization of strength development of bentonite and palm bunch ash concrete using fuzzy logic, International Journal of Sustainable Engineering, 14:4, 835-851, https://doi.org/10.1080/19397038.2021.1929549

[84] F. Althoey, P. O. Awoyera, K. Inyama et al., "Strength and microscale properties of bamboo fiber-reinforced concrete modified with natural rubber latex," Front. Mater.vol. 9, Article ID 1064885, 2022.

[85] S.-K. Lee, M.-J. Jeon, S.-S. Cha, and C.-G. Park, "Mechanical and permeability characteristics of latex-modified fiber reinforced roller-compacted rapid-hardening-cement concrete for pavement repair," Applied Science, vol. 7, no. 7, p. 694, 2017.

[86] Imoh Christopher Attah, Roland Kufre Etim, George Uwadiegwu Alaneme, David Ufot Ekpo. (2022). Scheffe's approach for single additive optimization in selected soils amelioration studies for cleaner environment and sustainable subgrade materials. Cleaner Materials, 100126, ISSN 2772-3976, https://doi.org/10.1016/j.clema.2022.100126

[87] M. Sriring, A. Nimpaiboon, S. Kumarn et al., "Film formation process of natural rubber latex particles: roles of the particle size and distribution of non-rubber species on film microstructure," Colloids and Surfaces A: Physicochemical and Engineering Aspects, vol. 592, no. 2, Article ID 124571, 2020

[88] G. C. Ezeokpube, G. U. Alaneme, I. C. Attah, I. M. Udousoro, and D. Nwogbo, "Experimental investigation of crude oil contaminated soil for sustainable concrete production," Architecture, Structures and Construction, 2022. https://doi.org/10.1007/s44150-022-00069-2

[89] Imoh Christopher Attah, George Uwadiegwu Alaneme, Roland Kufre Etim, Christopher Brownson Afangideh, Kufre Primus Okon & Obeten Nicholas Otu. Role of extreme vertex design approach on the mechanical and morphological behaviour of residual soil composite. Sci Rep (2023) 13:7933. https://doi.org/10.1038/s41598-023-35204-6

[90] Neelamegam, M., Dattatreya, J.K., Rajamane, N.P., Peter, J.A., and Gopalakrishnan, S. 2000. Development of durable cement concrete using natural rubber latex. Indian Concrete Journal, 74(8): 472– 479.

[91] Zhang, H.; Gou, M.; Liu, X.; Guan, X. Effect of rubber particle modification on properties of rubberized concrete. J. Wuhan Univ. Technol.-Mater. Sci. Ed. 2014, 29, 763–768.

[92] Gregory C. Ezeokpube, Isiguzo Edwin Ahaneku, George Uwadiegwu Alaneme, Imoh Christopher Attah, Roland Kufre Etim, Bamidele Charles Olaiya, and Iberedem Monday Udousoro (2022). Assessment of Mechanical Properties of Soil-Lime-Crude Oil-Contaminated Soil Blend Using Regression Model for Sustainable Pavement Foundation Construction. Advances in Materials Science and Engineering Volume 2022, Article ID 7207842, 18 pages https://doi.org/10.1155/2022/7207842

[93] Bala, M., Yussuf, A.A., and Mohammad, I. 2009. Making void-free cement-latex blend using morphology and thermal degradation analysis. Indian Concrete Journal, 83(11): 32–39.

[94] Jaafari, A.; Panahi, M.; Pham, B.T.; Shahabi, H.; Bui, D.T.; Rezaie, F.; Lee, S. Meta optimization of an adaptive neuro-fuzzy inference system with grey wolf optimizer and biogeography-based optimization algorithms for spatial prediction of landslide susceptibility. Catena 2019, 175, 430–445.

[95] Agor, C.D., Mbadike, E.M. & Alaneme, G.U. Evaluation of sisal fiber and aluminum waste concrete blend for sustainable construction using adaptive neuro-fuzzy inference system. Sci Rep 13, 2814 (2023). https://doi.org/10.1038/s41598-023-30008-0

[96] Naderpour, H., Rafiean, A. H., & Fakaharian, P. (2018). Compressive strength prediction of environmentally friendly concrete using artificial neural networks. Journal of BuildingEngineering, 16, 213–219

[97] Onyelowe KC, Alaneme GU, Onyia ME, Bui Van D, Diomonyeka MU, Nnadi E, Ogbonna C, Odum LO, Aju DE, Abel C, Udousoro IM, Onukwugha E (2021) Comparative modeling of strength properties of hydrated-lime activated rice-husk-ash (HARHA) modified soft soil for pavement construction purposes by artificial neural network (ANN) and fuzzy logic (FL). Jurnal Kejuruteraan 33(2) 2021: 365-384 https://doi.org/10.17576/jkukm-2021-33(2)-20

[98] Nihat, S. I. (2009). Estimation of swell index of fine grained soils using regression equations and artificial neural networks. Scientific Research and Essay, 4(10), 1047–1056.

[99] Obianyo, J.I., Udeala, R.C. & Alaneme, G.U. Application of neural networks and neuro-fuzzy models in construction scheduling. Sci Rep 13, 8199 (2023). https://doi.org/10.1038/s41598-023-35445-5

[100] Sarıdemir, M. Predicting the compressive strength of mortars containing metakaolin by artificial neural networks and fuzzy logic. Adv. Eng. Softw. 2009, 40, 920–927.

[101] Alaneme, G.U., Olonade, K.A. & Esenogho, E. Critical review on the application of artificial intelligence techniques in the production of geopolymer-concrete. SN Appl. Sci. 5, 217 (2023). https://doi.org/10.1007/s42452-023-05447-z

[102] Faeze Khademi, Sayed Mohammadmehdi Jamal, Neela Deshpande, Shreenivas Londhe, Predicting strength of recycled aggregate concrete using Artificial Neural Network, Adaptive Neuro-Fuzzy Inference System and Multiple Linear Regression, International Journal of Sustainable Built Environment, Volume 5, Issue 2, 2016, Pages 355-369, https://doi.org/10.1016/j.ijsbe.2016.09.003.

[103] Armaghani, D.J., Asteris, P.G. A comparative study of ANN and ANFIS models for the prediction of cement-based mortar materials compressive strength. Neural Comput & Applic 33, 4501–4532 (2021). https://doi.org/10.1007/s00521-020-05244-4

[104] 4. Jang, J. S. R. ANFIS: adaptive-network-based fuzzy inference system. IEEE Trans. Syst. Man Cybern. 23(3), 665–685 (1993)

[105] Alaneme, G.U., Mbadike, E.M., Attah, I.C., Udousoro, I.M. (2022). Mechanical behaviour optimization of saw dust ash and quarry dust concrete using adaptive neuro-fuzzy inference system. Innov. Infrastruct. Solut. 7, 122 (2022). https://doi.org/10.1007/s41062-021-00713-8

[106] Bi, Z.; Ma, J.; Pan, X.; Wang, J.; Shi, Y. ANFIS-Based Modeling for Photovoltaic Characteristics Estimation. Symmetry 2016, 8, 96

[107] Alaneme, G. U., Mbadike, E. M., Iro, U. I., Udousoro, I. M., & Ifejimalu, W. C. (2021). Adaptive neuro-fuzzy inference system prediction model for the mechanical behaviour of rice husk ash and periwinkle shell concrete blend for sustainable construction. Asian Journal of Civil Engineering (2021) 22:959–974 https://doi.org/10.1007/s42107-021-00357-0

[108] Neha, M., Ivan, G., & Arjan, B. (2016). Comparison of adaptive neuro-fuzzy inference system (ANFIS) and Gaussian processes for machine learning (GPML) algorithms for the prediction of skin temperature in lower limb prostheses. Journal of Medical Engineering and Physics, 38, 1083–1089. https://doi.org/10.1016/j. medengphy.2016.07.003

Ref.:
Nyah, Efiok Etim – **Onwuka**, David Ogbonna – **Alaneme**, George Uwadiegwu – **Onwuka**, Ulari Sylvi: *Systematic review of natural rubber latex modified concrete for eco efficient construction works*
Építőanyag – Journal of Silicate Based and Composite Materials, Vol. 75, No. 4 (2023), 154–164. p.
https://doi.org/10.14382/epitoanyag-jsbcm.2023.22

GUIDELINE FOR AUTHORS

The manuscript must contain the followings: title; author's name, workplace, e-mail address; abstract, keywords; main text; acknowledgement (optional)**; references; figures, photos with notes; tables with notes; short biography** (information on the scientific works of the authors).

The full manuscript should not be more than 6 pages including figures, photos and tables. Settings of the word document are: 3 cm margin up and down, 2,5 cm margin left and right. Paper size: A4. Letter size 10 pt, type: Times New Roman. Lines: simple, justified.

TITLE, AUTHOR

The title of the article should be short and objective.

Under the title the name of the author(s), workplace, e-mail address.

If the text originally was a presentation or poster at a conference, it should be marked.

ABSTRACT, KEYWORDS

The abstract is a short summary of the manuscript, about a half page size. The author should give keywords to the text, which are the most important elements of the article.

MAIN TEXT

Contains: materials and experimental procedure (or something similar), results and discussion (or something similar), conclusions.

REFERENCES

References are marked with numbers, e.g. [6], and a bibliography is made by the reference's order. References should be provided together with the DOI if available.

Examples:

Journals:

[6] Mohamed, K. R. – El-Rashidy, Z. M. – Salama, A. A.: In vitro properties of nano-hydroxyapatite/chitosan biocomposites. *Ceramics International.* 37(8), December 2011, pp. 3265–3271, http://doi.org/10.1016/j.ceramint.2011.05.121

Books:

[6] Mehta, P. K. – Monteiro, P. J. M.: Concrete. Microstructure, properties, and materials. *McGraw-Hill*, 2006, 659 p.

FIGURES, TABLES

All drawings, diagrams and photos are figures. The **text should contain references to all figures and tables**. This shows the place of the figure in the text. Please send all the figures in attached files, and not as a part of the text. **All figures and tables should have a title**.

Authors are asked to submit color figures by submission. Black and white figures are suggested to be avoided, however, acceptable.

The figures should be: tiff, jpg or eps files, 300 dpi at least, photos are 600 dpi at least.

BIOGRAPHY

Max. 500 character size professional biography of the author(s).

CHECKING

The editing board checks the articles and informs the authors about suggested modifications. Since the author is responsible for the content of the article, the author is not liable to accept them.

CONTACT

Please send the manuscript in electronic format to the following e-mail address: femgomze@uni-miskolc.hu and epitoanyag@szte.org.hu or by post: Scientific Society of the Silicate Industry, Budapest, Bécsi út 122–124., H-1034, HUNGARY

We kindly ask the authors to give their e-mail address and phone number on behalf of the quick conciliation.

Építőanyag – *Journal of Silicate Based and Composite Materials*, Quarterly peer-reviewed periodical of the Hungarian Scientific Society of the Silicate Industry, SZTE.
http://epitoanyag.org.hu